Iron and other transition metals in Patagonian riverborne and windborne materials: Geochemical control and transport to the southern South Atlantic Ocean

D. M. Gaiero,[1,2,*] J.-L. Probst,[2,3,†] P. J. Depetris,[1] S. M. Bidart,[4] and L. Leleyter[2,5,‡]

[1]CIGeS, FCEFyN, Universidad Nacional de Córdoba, Avda. Vélez Sàrsfield 1611, X50166CA Córdoba, Argentina
[2]Centre de Géochemie de la Surface (CNRS), 1, rue Blessig, 67084 Strasbourg Cedex, France
[3]Laboratoire des Mécanismes de Tranferts en Géologie, UMR CNRS/Université Paul Sabatier n° 5563, 38, rue des 36 Ponts, 31400 Toulouse, France
[4]Departamento de Geología, Universidad Nacional del Sur, Bahía Blanca, San Juan 670, 8000 Bahía Blanca, Argentina
[5]Equipe de Recherche en Physico-Chimie et Biotechnologies, Université de Caen, Bd. du Marechal Juin, 14032 Caen, Cedex, France

Abstract—The bulk of particulate transition metals transported by Patagonian rivers shows an upper crustal composition. Riverine particulate 0.5 N HCl leachable trace metal concentrations are mainly controlled by Fe-oxides. Complexation of Fe by dissolved organic carbon (DOC) appears to be an important determinant of the phases transporting trace metals in Patagonian rivers. In contrast, aeolian trace elements have a combined crustal and anthropogenic origin. Aeolian materials have Fe, Mn, and Al contents similar to that found in regional topsoils. However, seasonal concentrations of some metals (e.g., Co, Pb, Cu, and Zn) are much higher than expected from normal crustal weathering and are likely pollutant derived.

We estimate that Patagonian sediments are supplied to the South Atlantic shelf in approximately equivalent amounts from the atmosphere ($\sim 30 \times 10^6$ T yr^{-1}) and coastal erosion ($\sim 40 \times 10^6$ T yr^{-1}) with much less coming from the rivers ($\sim 2.0 \times 10^6$ T yr^{-1}). Low trace metal riverine fluxes are linked to the low suspended particulate load of Patagonian rivers, inasmuch most of it is retained in pro-glacial lakes as well as in downstream reservoirs. Based on our estimation of aeolian dust fluxes at the Patagonian coastline, the high nutrient-low chlorophyll sub Antarctic South Atlantic could receive 1.0 to 4.0 mg m^{-2} yr^{-1} of leachable (0.5 N HCl) Fe. Past and present volcanic activity in the southern Andes—through the ejection of tephra—must be highlighted as another important source of Fe to the South Atlantic Ocean. Based on the 1991 Hudson volcano eruption, it appears that volcanic events can contribute several thousand-fold the mass of "leachable" Fe to the ocean as is introduced by annual Patagonian dust fallout.

1. INTRODUCTION

Due to the thick ice sheet covering the surface of Antarctica, Patagonia is the only potentially important landmass for supplying terrigenous sediments to the South Atlantic Ocean (SAO) and the Southern Ocean. With 3000 km of coastal boundary, the fate of continental riverine and aeolian products should have an important effect upon the marine production in the coastal environment as well as in the adjoining open ocean. The Patagonian tableland adjacent to the Andes, is a huge glacial outwash plain with fluvioglacial channels, which is considered as one of the terrain-types acting as a major source of windblown dust (Pye, 1989). Owing to the extreme dryness of the air (relative humidity < 5%), intense dominant westerlies sweep the southern portion of South America and dust is eventually transported by the large-scale atmospheric circulation. The scarcity of rain near the Patagonian coast allows the dust to be transported into the sea instead of being removed from the atmosphere by precipitation near the sources.

The Southern Ocean has the greatest potential to affect atmospheric CO$_2$ levels (e.g., Falkowski et al., 1998). At present, this ocean is classified as a high-nutrient, low-chlorophyll (HNLC) system which, according to Martin et al. (1991), coincides with a region of particularly low supply of aeolian lithogenic dust, the main source of biologically available iron in regions far from continental sources (Duce, 1986). During all the Late Pleistocene glacial events, Patagonia was identified as a source of windblown dust deposited over East Antarctica (e.g., Basile et al., 1997). Patagonia could have supplied aeolian dust containing biologically available iron to the South Atlantic (Kumar et al., 1995), which in turn could have promoted, through sequestration, a decrease in atmospheric CO$_2$ concentrations during glacial periods (Barnola et al., 1987, Neftel et al., 1988).

Up to now the importance of this region for supplying terrigenous particles to the Southern Ocean and Antarctica has been a matter of speculation (e.g., Pierce and Siegel, 1979; de Baar et al., 1995; Kumar et al., 1995; Basile et al., 1997; Diekmann et al., 2000; Walter et al., 2000), as chemical and mineralogical information of transported material has been lacking. Hence, in this article we address the geochemical control and transport of riverborne and windborne trace elements from the southern portion of South America. The labile fraction of a group of trace metals (Fe, Mn, Pb, Cu, Ni, Cr, Zn, and Co) has been quantified in dissolved, suspended and, bed sediment matter, topsoils, and aeolian dust. We find the atmo-

* Author to whom correspondence should be addressed, at CIGeS, FCEFyN, Universidad Nacional de Córdoba, Avda. Vélez Sarsfield 299, 5000 Córdoba, Argentina (dgaiero@com.uncor.edu).
† Present address: Laboratorire des Mécanismes de Tranferts en Géologie, UMR CNRS/Université Paul Sabatier n° 5563, 38, rue des 36 Ponts, 31400 Toulouse, France.
‡ Present address: Equipe de Recherche en Physico-Chimie et Biotechnologies, Université de Caen, Bd. du Marechal Juin, 14032 Caen, Cedex, France.

spheric path to be more important than the riverine path in terms of metal fluxes as described below.

2. STUDY AREA

Continental Patagonia (between 38° to 52°S) covers an area of ~700,000 km². The climate is controlled by the westerlies dynamics, which blow from the Pacific Ocean, discharging most of their moisture on the Andes and continuing as dry winds to the east.

Only a small portion along the Andes (~15% of the total area) has a rainfall > 800 mm/yr. The dry steppe covers ~40% of Patagonia. Given these climatic and topographic characteristics for the region, it turns out that a limited area along the Andes, with steep slopes and heavy rainfall, is the active supplier of most of the weathered material that ultimately reaches the ocean. The geology is dominated by volcanic rocks (basalts, andesites, rhyolites), continental and, to a lesser extent, marine sediments. Metamorphic and plutonic rocks occur in relatively minor proportions. The rhyolites are overlain by Cretaceous and Cenozoic deposits, building up the foothills of the Precordillera and extending eastward into the Patagonian low land (Winslow, 1982).

Three essential factors are thought to be important for the occurrence of mineral aerosol transport: intense surface wind speed, low soil water content, and sparse vegetation cover (Tegen and Fung, 1994). In Patagonia, a paucity of precipitation and constant strong winds result in little movement of water through the soil. Westerly winds have mean monthly velocities of ~30 km/h and the maxima are recorded in October (southern spring) with velocities of over 100 km/h. Winds from the Atlantic Ocean are much calmer except during southeasterly storms (mostly in July) accounting for a frequency of 3%. Vegetation cover is only ~30%. The glaciers of the Southern Andes delivered enormous amounts of rock-flour and coarse debris during glacial ages. Thus, unconsolidated alluvial deposits of the last cold Pleistocene period were spread over the whole plateau, which is capped by a Holocene fluvial-deposit sandy layer (5–10 cm) (Rostagno and del Valle, 1988; Clapperton, 1993).

Eight main rivers drain this region and their combined drainage areas account for ~30% of the total Patagonian territory. The remaining 70% corresponds to closed basins and ephemeral smaller coastal drainage. The location and main features of each basin are shown in Table 1 and Figure 1. These river basins exhibit a spectrum of human impact. Reservoir lakes are present in the Colorado, Negro, and Chubut rivers. The main pollution problems are related to sewage effluents, agricultural runoff, oil extraction and transportation, and metal wastes located near harbors. Livestock breeding (mainly sheep) constitutes an important erosion agent all over Patagonia. The Negro and, to a lesser extent, the Chubut and Colorado River valleys are extensively farmed. Mining activities are of minor importance. Coal mining developed in the headwaters of the Gallegos River (Río Turbio) has generated abundant debris that is eventually wind-transported or is directly introduced into the river water.

3. MATERIAL AND METHODS

3.1. Sampling

River water and suspended particulate matter (SPM), river bed sediments, topsoil and aeolian dust samples were obtained from eight different surveys during 1995 to 1998. Sampling the land-ocean interface, along Patagonia's main road (RN 3) was emphasized. Some field trips, however, included sampling along the Andean range (RN 40), to sample the headwaters of rivers crossing Patagonia from west to east (Fig. 1). All the sampling sites in the Colorado, Negro, and Chubut rivers were located downstream of reservoir lakes.

3.1.1. Riverine Material

Composite water samples were taken from bridges by means of plastic sampling bottles, integrating three different points across the river width. The water samples were filtered in the field with a Nalgene polycarbonate filter holder through Milli-Q water pre-rinsed 47-mm diameter, 0.22-μm pore diameter HA filters (Millipore Corp.). The first 100 to 200 mL of filtrate was always discarded. Filtrates were stored in high-density polyethylene containers, which were previously washed with ultrapure 0.1 N HCl and rinsed with Milli-Q deionized water. The filtered samples were acidified in the field with ultrapure (Aldrich Chemical Corp., redistilled, 99.999+%) HNO_3 to pH 1 to 2 for trace element analyses. Previously weighted filters 47-mm diameter, 0.45-μm pore diameter HA filters (Millipore Corp.) were used to calculate seasonal suspended particulate matter (SPM) concentration of each river. With the purpose of acquiring enough material to run chemical analyses, SPM was preconcentrated by pressure filtration under 1.5 atm N_2 on to 142-mm diameter, 0.45-μm pore diameter HA filters (Millipore Corp.). Suspended particles were removed by submerging the filter in Milli-Q water and then employing an ultrasonic bath to liberate materials from filters. The vessel containing the water and particles was evaporated (50°C for ~24 h) to dryness and stored for further analyses. Submerged fine bed sediments were collected in duplicate from opposite riverbanks with plastic scoops during the field trips of May and December 1996.

There is a difference in pore-size between the filters employed to recuperate dissolved materials (0.22 μm) and those used to gather particulate matter (0.45 μm, 142 mm diameter). Our experience has shown that, due to the dominant mineralogical nature of Patagonian suspended load (mostly very fine-grained smectites), the filters rapidly changed their efficiency during filtration, retaining ultrafine particles after the first liter or so of fluid was filtered. Since quite large volumes (>10 L) were filtered for this work, the material comprised in the 0.45 to 0.22 μm gap was effectively retained on the 0.45-μm filters.

3.1.2. Atmospheric Fallout

Dust sampling devices were placed at selected spots: Bahía Blanca, Puerto Madryn, and Comodoro Rivadavia (Fig. 1). The Bahía Blanca site (~38°S), is located in southwestern Buenos Aires Province, and Puerto Madryn (~43°S) and Comodoro Rivadavia (~45°S) sites are located in northeast and southeast Chubut Province, respectively. The samplers used in each site were 40-cm deep, inverted epoxy-coated fiberglass pyramidal receptacles, with 0.25 cm² of collecting surface, as described by Orange et al. (1990). Atmospheric dust was collected from September 1998 until June 2000 at the Bahía Blanca site; from November 1998 to June 2000 at the Puerto Madryn site and from April 1999 to January 2000 at the Comodoro Rivadavia site.

The selected sites were high spots relative to the surrounding landscape. Dust samplers were installed ~5 m above the ground surface. At Comodoro Rivadavia the sampling device was set at a higher altitude (~35 m above the ground) to avoid contamination with particles from the irregular surrounding terrain. The sites were also selected to have a vegetated ground surface and be a maximum distance from any local anthropogenic dust source.

The dust deposited inside the container during a certain time period (e.g., 15–30 d) was rinsed from the walls with distilled water. In the laboratory, the sample suspensions were vacuum filtered through 0.45-μm pore-size filters (Millipore Corp.). The same procedure used for recuperate SPM was employed to prepare dust samples for further

Table 1. Features and physico-chemical parameters[a] for Patagonian Rivers.

Rivers	Ref.	Drainage area		Mean annual discharge ($m^3 s^{-1}$)	Population density (inhab. km^{-2})	Conductivity ($\mu S cm^{-1}$)	pH	DOC (mg L^{-1})	POC (% TSS)	SPM (mg L^{-1})	$SI_{calcite}$[b]	Ox_{sat}[c] (%)
		Total (km^2)	Upstream gauge (km^2)									
Colorado	RCOL	69,000	22,300	131	1.0	942 (837–1045)	8.1 (7.8–8.5)	1.2 (0.7–1.8)	2.8 (2.4–3.4)	45 (12–145)	0.3 (0–0.8)	97 (66–112)
Negro	RNEG	95,000	95,000	858	7.1	157 (116–192)	7.7 (6.5–8.5)	1.2 (0.9–1.4)	4.4 (2.0–6.6)	16 (5.6–28)	−1.0 [(−0.1)–(−2.1)]	86 (61–124)
Chubut	RCHU	57,400	31,680	42	3.5	295 (190–459)	7.7 (6.7–8.5)	2.1 (1.5–3.1)	2.5 (1.7–2.9)	62 (20–64)	−0.5 [(−1.6)–(0.4)]	81 (68–131)
Chico	RCHI	16,800	16,800	30	1.5	141 (105–208)	7.7 (7.0–8.5)	2.1 (1.4–3.7)	1.1 (0.7–1.8)	356 (129–668)	−1.0 [(−1.9)–(−0.2)]	85 (71–134)
Deseado	RDES	14,450	14,400	5	0.4	3730 (542–13703)	8.8 (8.4–9.3)	7.6 (4.0–10)	1.7 (1.1–2.6)	355 (37–930)	0.7 (0–1.5)	86 (56–105)
Santa Cruz	RSAN	24,510	24,000	691	0.2	41 (34–46)	6.3 (6.1–7.1)	0.8 (0.6–0.9)	2.4 (1.4–2.8)	23 (11–33)	−3.2 [(−3.8)–(−2.5)]	95 (65–122)
Coyle	RCOY	14,600	14,600	5	0.1	223 (145–266)	8.3 (7.6–10.2)	5.1 (3.4–7.0)	4.5 (3.4–5.4)	17 (8–24)	−0.2 [(−1.0)–(1.4)]	100 (85–140)
Gallegos	RGAL	6000	5100	34	1.3	112 (90–149)	7.1 (6.4–8.0)	6.7 (2.6–13)	7.8 (6.5–8.7)	32 (5–60)	−2.3 [(−2.6)–(−1.4)]	80 (47–96)

[a] Data represent the mean and figures in brackets are minimum and maximum values of at least six measurements taken on six different surveys of the rivers at they intersection with Patagonian main road, RN3.

[b] $SI_{calcite}$ = saturation index of calcite.
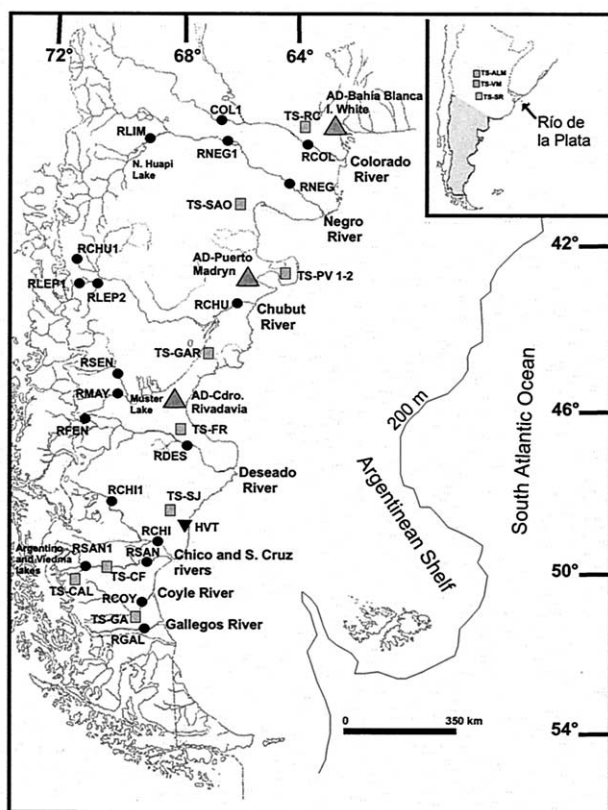
[c] Ox_{sat} = dissolved O_2 saturation.

Fig. 1. Map of Patagonia showing sampling points. Dots indicate water, suspended particulate matter, and bed sediments collected in different rivers. Boxes denote topsoil sampling locations and triangles denote aeolian dust sampling stations. See Table 4 for acronyms. Inset indicates topsoil sampling locations in central Argentina. In the Negro, Colorado and Chubut rivers the reservoirs are located upstream of the sampling sites. The remaining rivers do not have reservoir lakes in the drainage basins.

Table 2. Results for international geostandard OU-4 (Penmaenmawr microdiorite) and comparison with certified values. Elements are in ppm; oxides in wt%.

	Laboratory analysis	Certified values
Fe$_2$O$_3$	6.2 ± 0.1	5.82 ± 0.01
MnO	0.141 ± 0.003	0.140 ± 0.001
Al$_2$O$_3$	15.5 ± 0.2	14.83 ± 0.03
Zr	180 ± 3	195.1 ± 1.7
Ni	20.0 ± 0.3	21.0 ± 0.4
Co	12.2 ± 0.2	13.5 ± 0.3
Cr	55 ± 1	54.7 ± 1.0
Zn	70 ± 1	69.5 ± 0.8
Cu	25.0 ± 0.5	27.3 ± 0.5
Pb	12.8 ± 0.3	14.1 ± 0.4

Uncertainties represent ±1 standard deviation of the mean.

uncertainty better than 2%). Repeated blank analyses demonstrate that POC concentrations are not biased by any contamination.

Particulate samples (SPM, bed sediments, aeolian dust, and topsoils) were analyzed in bulk and as leachates. In each case, the whole sample was digested by means of the alkaline fusion method (Li$_2$B$_4$O$_7$, 1050°C, with HNO$_3$ digestion) and chemically analyzed for major (ICP-AES), minor, and trace components (ICP-MS). Standard curves of each element were constructed using international standards (BE-N-basalt, GS-N-granite, AN-G-anorthite, FK-N-feldspar) from the CRPG, Nancy, France. Following this methodology the precision based on five determinations was 2% for Al, Fe, and Mn and 5% for Zr, Pb, Cu, Co, Cr, Ni, and Zn. This technique was checked using the geostandard OU-4 (Penmaenmawr microdiorite) and the results obtained for the determined elements are reported in Table 2.

Two techniques were employed to study metal partitioning in Patagonian sediments: sequential extraction and single acid leaching. Selected Patagonian bed sediments and SPM were analyzed by a sequential extraction scheme designed to differentiate geochemical phases. Due to contamination problems in some of the reagents used in different sequential extraction steps, only Fe, Mn, Co, and Pb data from sequential extraction are presented here. Six phases were dissolved as follows (for further details see Leleyter and Probst, 1999): readily exchangeable (extracted with 1 mol/L magnesium nitrate); acid soluble carbonate (extracted with 1 mol/L sodium acetate, pH = 4.5), oxides of manganese (extracted with 0.1 mol/L hydroxylammonium chloride); amorphous Fe oxides (extracted with 0.2 mol/L ammonium oxalate-0.2 mol/L oxalic acid); crystallized oxides of Fe (extracted with 0.2 mol/L ammonium oxalate-0.2 mol/L oxalic acid-0.1 mol/L ascorbic acid); and metals associated with the organic matter (extracted with 0.02 mol/L HNO$_3$-35% H$_2$O$_2$-3.2 mol/L ammonium acetate/20% v/v HNO$_3$).

A less cumbersome single step acid leaching (0.5 N HCl) was applied to a large number of samples. This approach was intended to estimate the sum of the authigenically formed metal fraction in sediments since it purportedly extracts metals from all leachable sediment phases, without attacking aluminosilicate minerals (Agemian and Chau, 1976). To check the possible dissolution of aluminosilicate minerals, we analyzed Al and Si together with the leachable trace elements. The Al and Si concentrations from 13 Patagonian sediment samples were very low, constituting 3.2 ± 1.3 and 1.0 ± 0.5% respectively of their total bulk analysis. Analytical uncertainties on the determinations using 0.5 N HCl leaching techniques are estimated to be 3 to 10% for the investigated metals.

analysis. Due to large dilution factors and preservation problems the filtered waters were not routinely analyzed.

3.1.3. Topsoils

In connection with the aeolian dust aspect, a set of topsoil samples (upper 5 cm of the soil profile) were collected 300 to 400 km apart along the main route (RN 3) (Fig. 1). With the eventual purpose of correcting for the grain-size effect (i.e., larger grain-size fractions have a dilution effect on trace element concentrations) (Förstner and Wittman, 1981) both, bed sediments (from the May 1996 field trip) and topsoils were sieved with a 63-μm stainless steel mesh.

3.2. Analytical Methods

Dissolved Pb, Ni, Co, and, Cu were analyzed by inductively coupled plasma-mass spectrometry (ICP-MS; detection limit = 0.01 μg L^{-1} and uncertainty based on one relative standard deviation of replicates was < 5%). Dissolved Fe and Mn were analyzed by inductively coupled plasma-emission spectrometry (ICP-AES; detection limit = 10 μg L^{-1} for Fe and 0.5 μg L^{-1} for Mn, uncertainty of 2% were calculated similarly to above). Dissolved organic carbon (DOC) was measured in a Shimadzu TOC 5000 Analyzer. Each value represents a mean of three to five measurements (detection limit = 0.14 ppm and uncertainty of 2%). Particulate organic carbon (POC) was analyzed in material deposited on glass-fiber filters by means of a carbon, nitrogen, sulfur, and phosphorous analyzer (detection limit = 0.05 ppm and

3.3. Flux Estimation

3.3.1. Riverine Fluxes

Discharge data during the time of sampling were available for the main Patagonian rivers (i.e., Colorado, Negro, Chubut, Santa Cruz, and Gallegos: EVARSA-Evaluación de Recursos S.A., Buenos Aires, Argentina, http://www.mecon.gov.ar/hidricos/mapashidricos/mapageneral/htm, supplied the monthly river discharge data). For the less significant Patagonian rivers, namely, the Chico, Deseado, and Coyle rivers, there

Table 3. Measured and estimated leachable (0.5 N HCl) trace elements in suspended particulate matter (SPM). All data are expressed in $\mu g\ g^{-1}$.

		Fe	Mn	Pb	Ni	Co	Cu
Colorado River	Measured	3760	682	21	5.7	4.3	17
	Estimated[a]	3080	496	12	6.9	2.9	17
Deseado River	Measured	1710	270	9.5	2.4	1.7	6.4
	Estimated[a]	5000	346	3.7	4.8	2.6	9.4

[a] See section 3.3.1.

were no available discharge series for the period of sampling. Total discharge of these rivers represents only ~2% of the total discharge supplied by Patagonian rivers.

Metal fluxes (dissolved load, SPM, and bed sediments) were calculated by employing the available mean monthly discharge records corresponding to six different surveys (September 1995, May 1996, September 1996, December 1996 and 1997, and April 1998). To calculate the dissolved load transport rates we have averaged the interannual transport of trace metals as follows:

$$F_x = \frac{\sum C_{i(x)} Q_{mi}}{N} \quad (1)$$

Where F_x is the mean interannual flux of any chemical species, $C_{i(x)}$ is the concentration of element x during period i, Q_{mi} is the mean monthly discharge corresponding to the sampling period i, and N is the total number of sampling periods i. Fluxes for the Deseado, Chico and Coyle were estimated by substituting their mean annual discharge (Q_a) for Q_{mi} in Eqn. 1.

$$F_x = \frac{\sum C_{i(x)} Q_a}{N}$$

Particulate trace metal riverine inputs were estimated as follows:

$$F_{x(SPM)} = \frac{\sum C_x C_{i(SPM)} Q_{mi}}{N} \quad (2)$$

Where $F_{x(SPM)}$ is the total suspended particulate flux of element x, C_x is the mean concentration of element x in the suspended load and $C_{i(SPM)}$ is the concentration of the suspended load during sampling period i, and Q_{mi} is always the mean monthly discharge corresponding to i.

The concentration of an element in the suspended load was estimated from analyses of bed load material. Suspended matter transported by rivers is predominantly very fine material, consisting of silt- and clay-size fractions (~<20 μm). Since Patagonian rivers usually have very low SPM concentrations (see Table 1), it is very difficult to obtain enough material to determine a leachable fraction. Grain-size distributions of the Patagonian bed sediment fractions finer than 63 μm were measured. It is commonly true that the bulk of leachable trace metals contents are associated with finer grain sizes. If it is assumed that SPM has grain-size < 20 μm and it is primary leachable metal carrier, then a dilution factor (DF) can be applied to the bulk bed load analyses (Horowitz, 1991):

Concentration of mobile metal in SPM = (DF) (Chemical

concentration of metals in bed sediments) (3)

where

DF = 100/(100−percent size fraction > 20 μm) (4)

A comparison between leachable metals estimated in this way and measured values are given for the two suspended particulate matter samples in Table 3. The similarity between the approaches is evident. As will be discussed later, overestimation of the calculated Fe in the Deseado River could be linked to the major ion composition of its
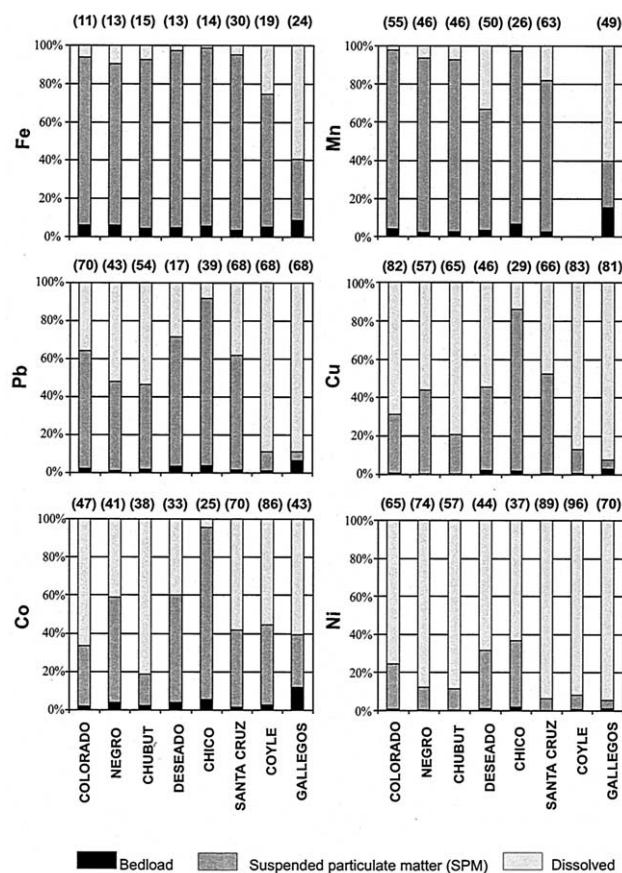

Fig. 2. Relative distribution of trace elements transported in leachable bed sediments, suspended particulate matter, and in dissolved form by Patagonian rivers. The numbers above stacked columns indicate the percentage leachable + dissolved to total metal export by each river. The concentration of an element in the suspended load was estimated from analyses of bed load material as described in section 3.3.1.

water which in turn could modify the speciation of metals. Underestimation of Pb concentrations could be related to a relatively higher abundance of Pb in the fine-grained carbonate fraction of suspended particulate matter. Detrital carbonate found in bed sediments samples is coarser and less reactive. Given the general agreement, it appears valid to approximate suspended particulate matter composition in sites where no such information is available. We applied this approach to estimate the leachable metals transported in the SPM of each Patagonian river (Fig. 2).

Table 4 shows the total trace element concentrations in Patagonian particulate materials. Fluxes of leachable metals transported by bed sediments were calculated using the transition metals concentrations for each Patagonian river bed sediment sample (Table 5) and, by assuming that 10% of the SPM flux is the mass transported along the river bed-water interface. This assumption is consistent with the proportion of SPM representing bedload as reported in the literature (Milliman and Meade, 1983; Pinet and Souriau, 1988).

3.3.2. Aeolian Dust Fluxes

Very few individual aeolian dust samples consisted of enough material (minimum of 200 mg) for chemical analyses. Only 14 of the 62 samples collected from different sampling spots were large enough. When the amount of material was lower than the minimum required for analysis, samples from two consecutive periods were grouped together. In the case of the Comodoro Rivadavia site, 8 samples from April to

Table 4. Total trace element concentrations in Patagonian particulate materials. All data are expressed in $\mu g\ g^{-1}$ except Al and Fe in wt%. Sample locations corresponds to Figure 1.

Sample I.D.	Sample type and localization	Al	Zr	Fe
	Bed Sediment <63 μm size fraction[a]			
RCOL1	Colorado R. (La Japonesita)	7.70 ± 0.04	417 ± 18	4.6 ± 0.1
RLIM	Limay River (Nahuel Huapi outlet)	8.26 ± 0.07	267.9 ± 0.1	4.4 ± 0.1
RNEG1	Negro River (Chelforò)	8.1 ± 0.2	379 ± 18	4.86 ± 0.05
RLEP1	Lepà R. (Gualjaina)	8.8	211	4.9
RLEP2	Lepà R. (RN 40)	8.8	193	5.5
RMAY	Mayo R. (Río Mayo)	8.3 ± 0.4	372 ± 36	5.2 ± 0.6
RSEN	Senguer R. (RN 40)	8.1 ± 0.2	1111	3.9 ± 0.5
RCHU1	Chubut River (El Maitén)[b]	8.97 ± 0.03	246 ± 25	5.0 ± 0.4
RFEN	Fénix River (Perito Moreno)[b]	8.9	207	4.5
RCHI1	Chico River (Tamel Aike)	8.1	698	5.5
RSAN1	Santa Cruz R. (Ch. Fuhr)[b]	6.9 ± 0.1	596 ± 86	3.56 ± 0.01
RCOL	Colorado R. (Rio Colorado)	7.8 ± 0.3	301 ± 11	4.30 ± 0.05
RNEG	Negro River (Gral. Conesa)	8.65 ± 0.04	261 ± 14	5.2 ± 0.2
RCHU	Chubut River (Trelew)	8.3 ± 0.2	382 ± 40	3.81 ± 0.05
RDES	Deseado River (Jaramillo)	7.1 ± 0.1	232 ± 6	3.3 ± 0.2
RCHI	Chico River (Río Chico)	7.8 ± 0.4	211 ± 7	3.6 ± 0.5
RSAN	Santa Cruz R. (Cte. Piedrabuena)	7.9 ± 0.6	306 ± 16	4.1 ± 0.5
RGAL	Gallego River (Güer Aike)	7.8 ± 0.4	161 ± 7	3.8 ± 0.8
	Suspended particulate matter (SPM)[c]			
RCOL	Colorado R. (R. Colorado)	7.4 ± 0.3	144 ± 20	2.8 ± 0.3
RNEG	Negro River (Gral. Conesa)	6.8 ± 1.4	145 ± 10	4.12 ± 0.03
RCHU	Chubut River (Trelew) during flood	8.8	202	3.8
RCHU	Chubut River (Trelew)	7.3 ± 0.2	201 ± 3	4.2 ± 0.9
RFEN	Fénix River (Perito Moreno)	8.5	177	4.1
RDES	Deseado River (Jaramillo)	7.9 ± 0.6	206 ± 12	4.2 ± 0.2
RCHI1	Chico River (Tamel Aike)	9.5	156	4.9
RCHI	Chico River (Río Chico)	9.7 ± 0.3	157 ± 14	5.2 ± 0.5
RSAN	Santa Cruz R. (Cte. Piedrabuena)	8.2 ± 0.2	153 ± 2	4.2 ± 0.2
RCOY	Coyle River (Río Coyle)	8.9	155	5.2
RGAL	Gallego River (Güer Aike)	7.0	na	1.6
	Aeolian dust (AD)-dates of collects			
AD-B. Blanca	Bahía Blanca-Aug'97 to Mar'98	7.1	174	4.6
AD-B. Blanca	Bahía Blanca-Mar to Oct'98	7.5	186	4.0
AD-B. Blanca	Bahía Blanca-Set to Nov'98	8.5	190	4.0
AD-B. Blanca	Bahía Blanca-Dec'98 to Feb'99	8.5	188	4.6
AD-B. Blanca	Bahía Blanca-Set'99	6.7	153	3.4
AD-I. White	Ing, White-Set'97 to Jul'98	7.8	179	4.3
AD-I. White	Ing, White-Jul to Dec'98	7.7	197	4.2
AD-P. Madryn	Puerto Madryn-May to Nov'98	7.0	224	3.1
AD-P. Madryn	Puerto Madryn-Jan to Feb'99	6.9	170	3.5
AD-P. Madryn	Puerto Madryn-Feb to Mar'99	8.3	217	3.7
AD-P. Madryn	Puerto Madryn-May'99	7.3	252	3.1
AD-P. Madryn	Puerto Madryn-Jun to Jul'99	9.4	209	2.9
AD-P. Madryn	Puerto Madryn-Set to Oct'99	7.2	242	3.4
AD-Cdro. Rivadavia	Comodoro Rivadavia- Apr to Jul'99	6.7	156	3.8
	Topsoils (all duplicates)			
	Patagonia			
TS-RC	Río Colorado	7.8 ± 0.4	286 ± 98	4.9 ± 0.6
TS-SAO	San Antonio Oeste	8.1 ± 0.8	240 ± 4	5.3 ± 0.4
TS-PV	Península de Valdéz-1	8.0 ± 0.2	320 ± 13	4.89 ± 0.01
TS-PV	Península de Valdéz-2	8.0 ± 0.1	375 ± 15	4.29 ± 0.01
TS-GAR	Garrayalde (RN 3)	7.9 ± 0.1	453 ± 56	3.95 ± 0.05
TS-FR	Fitz Roy (RN 3)	5.8 ± 0.6	379 ± 58	3.8 ± 0.1
TS-SJ	San Julián	7.7 ± 0.3	276 ± 83	4.2 ± 1.0
TS-GA	Güer Aike	5.69 ± 0.03	303 ± 57	3.2 ± 0.2
TS-CAL	El Calafate[b]	7.3 ± 0.2	248 ± 27	3.3 ± 0.5
TS-CF	Charles Fuhr[b]	7.96 ± 0.04	1141 ± 77	4.58 ± 0.04
	Central Argentina			
TS-ALM	Almafuerte	8.0 ± 0.2	381 ± 56	3.31 ± 0.05
TS-VM	Vicuña Mackenna	7.5 ± 0.1	890 ± 170	6.4 ± 1.2
TS-SR	Santa Rosa	8.3 ± 0.1	248 ± 23	3.62 ± 0.01
HVT-1	Hudson volcanic tephra	8.7	355	4.5
HVT-2	Hudson volcanic tephra[d]	8.7	338	4.6

Some trace element concentrations in bed sediment and SPM were taken from Gaiero et al. (2002).

[a] Mean concentration (duplicated samples) ±1 standard deviation.

[b] Samples representative of glacial deposits.

[c] Except for the SPM of the Chubut (during flood), Fénix and Chico (at T. Aike) rivers, all the data are mean concentrations of two surveys. Uncertainties represent ± 1 standard deviation of the mean.

[d] From Déreulle and Bourgois (1993).

nd = not detected na = not analyzed.

Mn	Ni	Co	Cr	Zn	Cu	Pb
833 ± 11	20.5 ± 0.7	19.0 ± 0.7	48.5 ± 0.7	86.0 ± 1.4	25.5 ± 3.5	15.66 ± 0.05
983 ± 55	21.7 ± 1.4	16.5 ± 0.7	57.5 ± 0.7	86.5 ± 0.7	29.7 ± 0.3	20.5 ± 0.5
883 ± 11	17.0 ± 2.8	19.0 ± 0.7	62 ± 18	97.9 ± 0.1	27.9 ± 0.1	20.6 ± 3.6
968	27	17	32	66	25	18
1140	31	19	59	75	34	14
1180 ± 82	17.1 ± 1.4	21.0 ± 0.7	75.0 ± 4.2	86.0 ± 2.8	15.95 ± 0.07	16.5 ± 3.3
1120 ± 310	8.5 ± 0.7	19.1 ± 3.5	45 ± 10	68.0 ± 2.8	4.0 ± 2.8	19.2 ± 8.2
1040 ± 130	27.0 ± 1.4	18.0 ± 1.4	75.0 ± 7.1	101 ± 5	25.5 ± 0.7	18.8 ± 1.3
1060	20	17	53	82	22	13
1020	17	21	53	97	20	17
821 ± 88	24.5 ± 3.5	18.0 ± 1.4	70.5 ± 0.7	78.5 ± 2.1	17.93 ± 0.07	16.36 ± 0.02
798 ± 22	18.0 ± 1.4	16.5 ± 0.7	44.5 ± 2.1	80.5 ± 7.8	23.5 ± 2.1	15.6 ± 1.3
1050 ± 5	20.5 ± 0.7	19.8 ± 0.1	38.5 ± 3.5	101 ± 1	35.5 ± 2.1	21.4 ± 0.9
736 ± 13	13.95 ± 0.07	14.5 ± 0.7	66.5 ± 0.7	59.5 ± 2.1	12.5 ± 0.7	15.6 ± 0.3
743 ± 55	13.5 ± 0.7	11.9 ± 0.1	24.5 ± 0.7	61.0 ± 7.1	15.0 ± 4.2	19.9 ± 0.5
	16.9 ± 0.1	14.5 ± 0.7	41.5 ± 0.7	76.5 ± 9.2	19.0 ± 5.7	24 ± 15
755 ± 16	23.7 ± 0.3	16.0 ± 1.4	52.5 ± 3.5	91.5 ± 3.5	23.5 ± 2.1	45 ± 14
1430 ± 860	21.0 ± 1.4	15.5 ± 4.9	38.5 ± 0.7	89 ± 36	31 ± 24	34 ± 26
867 ± 11	20.5 ± 3.5	12.0 ± 1.4	69 ± 39	125 ± 67	31 ± 10	21.3 ± 2.1
2400 ± 1000	38.5 ± 1.4	16.0 ± 5.7	49 ± 22	320 ± 200	160 ± 180	46 ± 19
891	21	17	42	110	33	16
1360 ± 220	28 ± 11	14.0 ± 2.1	45 ± 7	162 ± 32	39 ± 10	26.4 ± 7.5
1150	na	na	31	84	39	26
850 ± 310	20.0 ± 5.7	15.0 ± 3.5	27.0 ± 3.5	112 ± 48	24.0 ± 5.0	20.1 ± 9.0
867	8	13	33	117	35	
740 ± 60	22.0 ± 7.0	17.0 ± 2.8	53 ± 16	227 ± 68	49 ± 24	26.7 ± 4.9
1100 ± 130	34	19.0 ± 1.4	75 ± 20	305 ± 81	70 ± 39	68 ± 13
860	20	20	43	126	39	15
618	10	8	28	124	18	9
643	28	14	57	5697	109	381
581	17	13	35	1040	41	55
635	14	11	49	315	35	53
759	74	19	37	1236	66	71
666	25	17	40	718	219	150
503	27	13	57	312	61	164
798	30	17	49	522	120	224
581	19	244	34	110	47	95
596	18	181	95	106	29	125
681	27	204	40	2105	260	147
542	17	150	37	100	36	84
573	22	80	39	126	23	76
604	25	128	45	205	58	84
728	25	1463	49	735	122	80
980 ± 130	15.5 ± 0.7	20.5 ± 3.5	39.5 ± 7.8	91 ± 10	50 ± 11	17.4 ± 0.3
980 ± 190	18.5 ± 3.5	21.5 ± 2.1	43.5 ± 0.7	97 ± 11	53 ± 10	22.8 ± 5.9
960 ± 10	13.95 ± 0.07	19.95 ± 0.07	45.95 ± 0.07	89 ± 2.8	33.0 ± 2.8	13.8 ± 0.8
880 ± 20	13.0 ± 2.1	19.5 ± 0.7	52.95 ± 0.07	78.5 ± 0.7	29.5 ± 2.1	13.3 ± 0.1
956 ± 5	12.95 ± 0.07	22.5 ± 0.7	63.5 ± 9.2	63.5 ± 9.2	29.5 ± 2.1	13.4 ± 0.2
620 ± 85	18.0 ± 5.0	15.3 ± 0.6	38.0 ± 2.8	61.0 ± 8.5	16.95 ± 0.07	15.4 ± 3.1
840 ± 110	13.0 ± 1.4	18.95 ± 0.07	43.5 ± 5.0	78 ± 19	22.0 ± 7.1	14.1 ± 2.0
879 ± 27	15.0 ± 1.4	15.0 ± 1.4	47.5 ± 9.2	82 ± 13	21.95 ± 0.07	7.2 ± 0.1
1170 ± 82	13.0 ± 2.8	20.0 ± 1.4	40 ± 10	63 ± 12	19.0 ± 1.4	10.5 ± 0.1
1000 ± 22	26.5 ± 0.7	26.5 ± 0.7	91 ± 16	128 ± 6	30.0 ± 1.4	24.4 ± 0.6
662 ± 16	17.0 ± 2.8	17.0 ± 0.1	47 ± 11	84 ± 17	35.5 ± 7.8	16.95 ± 0.07
910 ± 93	31.5 ± 3.5	16.8 ± 0.8	83 ± 6	137 ± 4	36.0 ± 2.8	16.9 ± 0.8
670 ± 5	10.95 ± 0.07	15.5 ± 0.7	31.5 ± 0.7	69.0 ± 2.8	30.5 ± 0.7	16.2 ± 1.5
1390	3.0	17	48	97	nd	14
1470	6.0	nd	12	93	9.0	na

Table 5. Leachable (acid-extracted metals with 0.5 N HCl) and dissolved trace metals in different Patagonian sediment-types and river waters. All the sediment data expressed in $\mu g\ g^{-1}$. Dissolved concentrations are expressed in $\mu g\ L^{-1}$. The numbers in brackets represent the proportion of leachable metals relative to their total concentrations in each sample.

Samples I.D.	Sample type and localization	Fe	Mn	Ni	Co	Cu	Pb
	Bed Sediment <63 μm size fraction						
RLIM	Limay River (Nahuel Huapi outlet)	3250 (7.0)	182 (19)	1.7 (8.0)	1.3 (8.0)	4.5 (15)	4.2 (21)
RCHU1	Chubut River (El Maitén)	5100 (10)	234 (25)	2.5 (9.0)	2.7 (14)	7.7 (30)	4.7 (26)
RFEN	Fénix River (Perito Moreno)	3610 (8.0)	311 (29)	2.7 (14)	2.8 (16)	4.2 (19)	2.4 (18)
RCHI1	Chico River (Tamel Aike)	3710 (7.0)	223 (22)	1.9 (11)	2.7 (13)	4.3 (22)	5.3 (31)
RSAN1	Santa Cruz R. (Ch. Fuhr)	4650 (13)	208 (24)	3.4 (15)	3.6 (19)	3.8 (21)	4.3 (26)
RMAY	Mayo R. (Rio Mayo)	3110 (6.0)	290 (26)	1.7 (10)	2.6 (13)	3.0 (19)	1.9 (10)
RSEN	Senguer R. (RN 40)	4270 (10)	183 (14)	1.3 (14)	3.5 (17)	3.5 (22)	2.6 (20)
RCOL	Colorado R. (R. Colorado)	2100 (5.0)	202 (26)	2.6 (15)	1.8 (11)	5.5 (25)	4.1 (27)
RNEG	Negro River (Gral. Conesa)	3650 (7.0)	262 (25)	2.7 (14)	3.2 (16)	7.3 (20)	3.3 (15)
RCHU	Chubut River (Trelew)	2970 (8.0)	183 (25)	1.7 (7.0)	1.4 (5.0)	2.6 (15)	3.2 (19)
RDES	Deseado River (Jaramillo)	2500 (7.0)	168 (24)	1.8 (14)	1.2 (10)	4.2 (23)	2.3 (11)
RCHI	Chico River (Río Chico)	4510 (11)	152 (20)	2.2 (13)	2.6 (19)	2.9 (19)	4.3 (32)
RSAN	Santa Cruz R. (Cte. Piedrabuena)	5100 (13)	200 (26)	3.7 (15)	3.3 (22)	5.8 (23)	9.1 (26)
RCOY	Coyle R. (RN 3)[a]	3790 (9.0)	857	10 (43)	5.7 (47)	5.4 (23)	3.1 (18)
RGAL	Gallego River (Güer Aike)	7690 (20)	860 (47)	4.0 (19)	6.3 (34)	21 (47)	25 (53)
	Suspended particulate matter (SPM)						
RDES	Deseado River (December 1997)	1710 (4.0)	270 (40)	2.4 (15)	1.7 (11)	6.4 (32)	14 (70)
RCOL	Colorado River (December 1997)	3760 (10)	682 (54)	5.7 (7.0)	4.3 (31)	17 (37)	21 (51)
	Aeolian dust (AD)						
AD-I. White	IW-Set'97 to Jul'98	4280 (10)	40 (8.0)	2.9 (11)	1.2 (9.0)	19 (32)	66 (41)
AD-I. White	IW-Jul to Dec'98	4120 (10)	286 (36)	7.7 (26)	4.2 (24)	76 (64)	120 (54)
AD-P. Madryn	PM-May to Nov'98	2170 (7.0)	155 (27)	4.5 (27)	228 (93)	18 (37)	65 (69)
	Topsoils (TS)						
TS-RC	Rio Colorado	322 (0.6)	159 (15)	1.6 (10)	2.3 (10)	2.4 (6.0)	3.1 (18)
TS-SAO	San Antonio Oeste	100 (0.2)	114 (10)	1.9 (9.0)	1.9 (8.0)	1.8 (3.0)	2.2 (12)
TS-GAR	Garrayalde A (RN 3)	679 (2.0)	139 (14)	2.6 (20)	3.8 (17)	4.5 (16)	1.7 (13)
TS-GAR	Garrayalde B (RN 3)	853 (2.0)	106 (11)	2.6 (20)	3.4 (15)	2.6 (8.0)	1.5 (11)
TS-SJ	San Julián	249 (1.0)	249 (27)	2.7 (22)	4.4 (23)	4.3 (25)	2.4 (19)
TS-GA	Güer Aike A	900 (3.0)	231 (27)	2.5 (18)	1.7 (12)	3.0 (14)	2.2 (30)
TS-GA	Güer Aike B	769 (2.0)	228 (25)	2.5 (16)	1.7 (11)	2.7 (12)	2.4 (33)
TS-CAL	El Calafate A	979 (3.0)	165 (15)	3.2 (22)	4.2 (22)	4.1 (20)	3.0 (28)
TS-CAL	El Calafate B	1180 (4.0)	204 (17)	2.4 (22)	3.1 (15)	3.4 (19)	2.7 (26)
HVT-1	Hudson volcanic tephra	1220 (3.0)	49 (4.0)	1.4 (23)	nd	nd	nd
	Dissolved (filtered w/ 0.22μm)						
RLIM	Limay River (Nahuel Huapi outlet)	12	nd	0.08	nd	0.52	0.21
RCHU1	Chubut River (El Maitén)	19	nd	nd	0.06	nd	0.10
RSAN1	Santa Cruz R. (Ch. Fuhr)	7.5	2.6	1.7	0.38	0.65	0.52
RCHI1	Chico River (Tamel Aike)	10	2.4	nd	nd	nd	nd
RCOL	Colorado R. (R. Colorado)[b]	14 (<10–49)	1.8 (<0.5–4.0)	1.8 (0.29–5.2)	0.44 (0.11–0.64)	3.0 (2.1–5.8)	0.72 (0.15–1.7)
RNEG	Negro R. (Gral. Conesa)[b]	11 (<10–19)	1.6 (<0.5–2.3)	1.7 (<0.01–5.2)	0.08 (<0.01–0.23)	1.4 (<0.01–4.3)	0.29 (0.11–0.52)
RCHU	Chubut R. (Trelew)[b]	22 (<10–19)	1.0 (<0.5–5.0)	1.9 (<0.01–5.5)	0.41 (<0.01–1.6)	2.0 (<0.01–6.3)	0.54 (<0.01–0.78)
RDES	Deseado R. (Jaramillo)[b]	42 (11–133)	3.2 (<0.5–9.0)	1.0 (<0.01–10)	0.60 (<0.01–1.9)	3.2 (<0.01–7.1)	0.42 (<0.01–0.78)
RCHI	Chico R. (Río Chico)[b]	42 (20–73)	2.5 (<0.5–4.5)	1.5 (<0.01–5.5)	0.11 (<0.01–0.23)	2.0 (<0.01–5.6)	0.56 (0.33–0.86)
RSAN	Sta. Cruz R. (Cte. Piedrabuena)[b]	16 (<10–52)	3.0 (<0.5–7.0)	2.6 (<0.01–6.6)	0.21 (<0.01–1.0)	0.70 (<0.01–2.1)	0.45 (0.08–1.3)
RCOY	Coyle R. (RN 3)[b]	54 (<10–150)	1.3 (<0.5–4.0)	2.2 (<0.01–4.4)	0.26 (<0.01–0.41)	1.7 (<0.01–3.6)	0.55 (0.32–1.7)
RGAL	Gallego R. (Güer Aike)[b]	155 (52–374)	11 (5.0–25)	1.3 (<0.01–4.0)	0.14 (<0.01–0.25)	2.2 (<0.01–4.5)	1.1 (0.33–2.4)

[a] Percentage calculated using total metal concentration from Table 4.

[b] Mean of seasonal samples. Numbers in brackets are minimum and maximum values of at least six measurements taken on six different surveys of the rivers at they intersection with Patagonian main road, RN3.
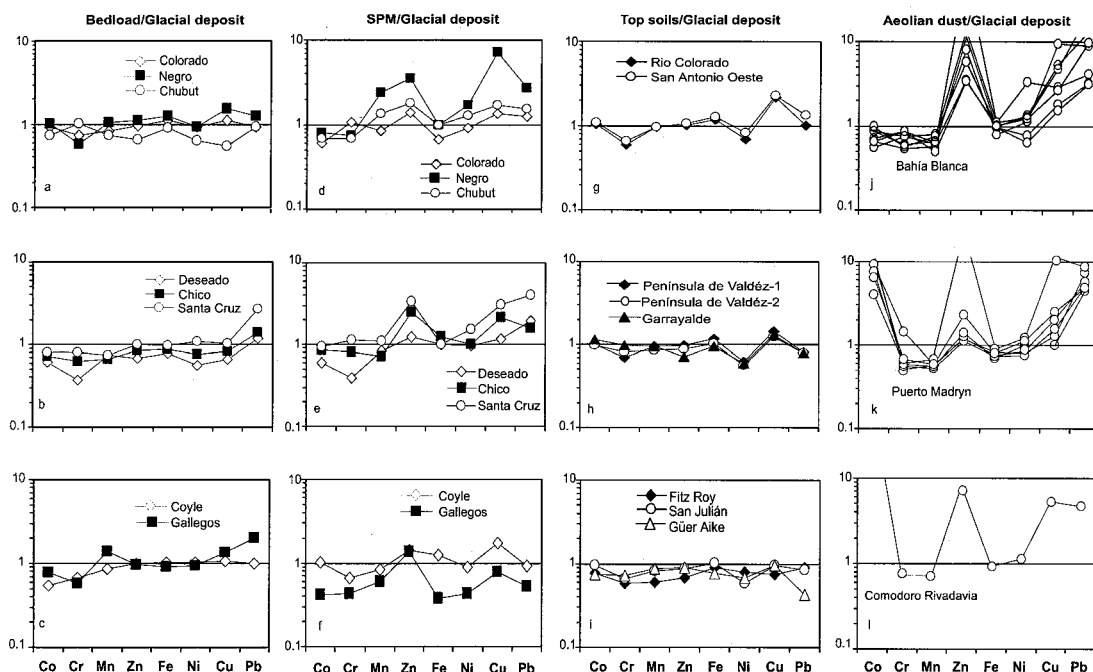
na = not analyzed, nd = not detected.

Fig. 3. Glacial deposit-normalized bulk trace elements abundance in river bed sediments and suspended sediments, topsoils, and aeolian dust patterns from Patagonia.

July 1999 accounted for only 300 mg, so that they were grouped together and analyzed as a composite fallout. Fluxes were estimated using the trace metal composition of the corresponding aeolian dust mass deposited during the period under consideration.

4. RESULTS AND DISCUSSION

4.1. Patagonian Upper Crust Trace Element Signature

Materials from large rivers and loess (Taylor et al., 1983), and glacial deposits (Goldschmidt, 1933), represent valuable samples as they integrate the lithological and chemical diversity of the continental crust. In Patagonia, Quaternary glacial deposits outcrop in a long and narrow area along the eastern slope of the Andes. Five such bed sediments and topsoil samples located in remote areas (Fig. 1; references in Table 4) were taken as representative of the chemistry of glacial deposits. The chemical compositions of all sediments were normalized to this composite sample (Fig. 3).

Flat distributions demonstrate the local upper crustal composition of Patagonian bed sediments and topsoils (Fig. 3). Patagonian topsoils samples are in general fluvio-glacial deposits with heterogeneous grain-size and mineralogical composition. With little local variation, trace element distributions in topsoils samples are very similar to the glacial deposit composition (Figs. 3g–3i). This is in agreement with numerous investigations (see summary by Ure and Berrow, 1982), showing that the total element content of a soil is basically determined by slight weathering of the parent materials.

Glacial deposit-normalized suspended load and aeolian dust samples display much more variability than bed sediments and topsoils samples (Fig. 3). Their patterns may be explained by the predominance of fine grain-size material in the suspended load and aeolian dust samples having a higher capacity of adsorption. On the global scale (but also particularly for Patagonian rivers), riverine suspended matter originates mainly from mountainous areas where the concentrations of elements such as Cu, Pb and Zn tend to be higher (Wilson and Laznicka, 1972). Based on data from unpolluted central Patagonian rivers, with the probable exception of the Negro River, the enrichment in Pb, Zn and Cu found in SPM can be attributed to the scavenging efficiency of fine particles, which is especially evident in areas of high natural background.

The average Fe concentration of Patagonian aeolian dust samples was 3.7% or similar to typical mineral aerosol (3.5%; Duce, 1986). This concentration is slightly less than the glacial deposit Fe abundance (4.2%). Industrial particulate emissions and fossil-fuel burning (Lantzy and Mackenzie, 1979) could explain the extremely high concentrations of Pb, Zn, Cu and Co in aeolian dust samples (Figs. 3j–3l). Topsoils do not appear to be probable sources for these metals in dust. In the Patagonian study region, aeolian erosion appears to be a dominant process over deposition, as indicated by thousands of deflation hollows developed in the landscape (Iriondo, 2000). Aeolian dust seems to have little influence on the chemical composition of riverine materials (Fig. 3).

Clay minerals from Patagonian sediments can serve as a substrate for the precipitation and flocculation of organics and secondary minerals in rivers (i.e., hydrous Fe and Mn oxides) (Jenne, 1976). The bulk concentration of Fe, Cu, and Pb in our suspended particulate matter and bed sediment samples show a clear tendency to increase with the percentage of clay minerals, though this association is less evident for Mn. This observation is in agreement with Jenne (1968) who found a positive correlation between free-oxides and clay contents but no correlation between free-manganese oxides and clay minerals.

Similarly to clay minerals, heavy minerals contain significantly high metal contents and frequently exhibit a close relationship with specific source materials of regional nature (Förstner and Wittman, 1981). Since these minerals were identified in the fine sand size-fraction of bedload samples their contribution to the trace element pool in the silt- and clay-size fraction should be taken into account. Therefore, the possible association of trace elements with heavy minerals was tested using Zr concentrations as a proxy variable. Significant correlations of Co and Cr with Zr concentrations were observable in bed sediments ($r = 0.74$ for Cr, and $r = 0.75$ for Co, $p < 0.01$). This observation is in agreement with the apparent depletion of these metals (mainly Cr) found in some glacial deposit-normalized bedload samples (Fig. 3). This behavior indicates that light minerals could have been enriched through sorting over heavy ones during their transport to distal areas.

4.2. The Geochemical Control of Trace Elements in Patagonia

4.2.1. Riverborne Materials

4.2.1.1. Major phases controlling particulate trace elements. Trace elements transported in the aquatic environment by the labile particulate fraction along with the dissolved phase are the most important in terms of their mobility and bio-availability. The relative transport of dissolved and leachable metals by Patagonian rivers as compared to the total metal transport (Fig. 2), indicates that a higher proportion of the elements (with the exception of Fe) is delivered to the coastal zones in their mobile form. For most rivers, Fe and Mn are exported mainly in the SPM fraction, thus reflecting their tendency to occur as oxyhydroxide coatings on various minerals and dispersed particles (e.g., Salomons and Förstner, 1984). Probably due to an anthropogenic origin, dissolved Pb has a rather high mean concentration in Patagonian rivers (i.e., 0.60 ± 0.20 μg L^{-1}) (Table 4). This could be explained by the extended usage of lead-containing gasoline in Argentina. In general, a similar quantity of Pb and Cu are delivered by the dissolved and particulate phases. Lead has a strong tendency to be adsorbed by particle surfaces and Cu has a marked tendency to form inorganic and organic complexes (Stumm and Morgan, 1996). On the contrary, Ni and Co have a relatively weaker tendency to form complexes. They tend to occur, to a significant extent, as free cations (Stumm and Morgan, 1996), which is consistent with their transport primarily in the dissolved load of Patagonian rivers (Fig. 2).

Selected bed sediments and SPM samples analyzed by means of chemical sequential extraction, allow us to further investigate operationally defined phases in the solid form transported in Patagonian rivers. There is a general consensus that within surficial sediments, the three most important geochemical components in trace element control are the oxides of Mn and Fe, and organic matter (e.g., Gibbs, 1977; Bendell-Young and Harvey, 1992; Tessier et al., 1996; Dong et al., 2000). Our data (Fig. 4) indicate that trace elements are mainly bound to the Fe-oxide fraction (average 25%) and, to a lesser extent, to the organic matter fraction (average 6%). Manganese oxides play a relatively minor role in trace element adsorption.

Due to complex physical, chemical and biologic processes, a major fraction of trace metals introduced into the aquatic en-
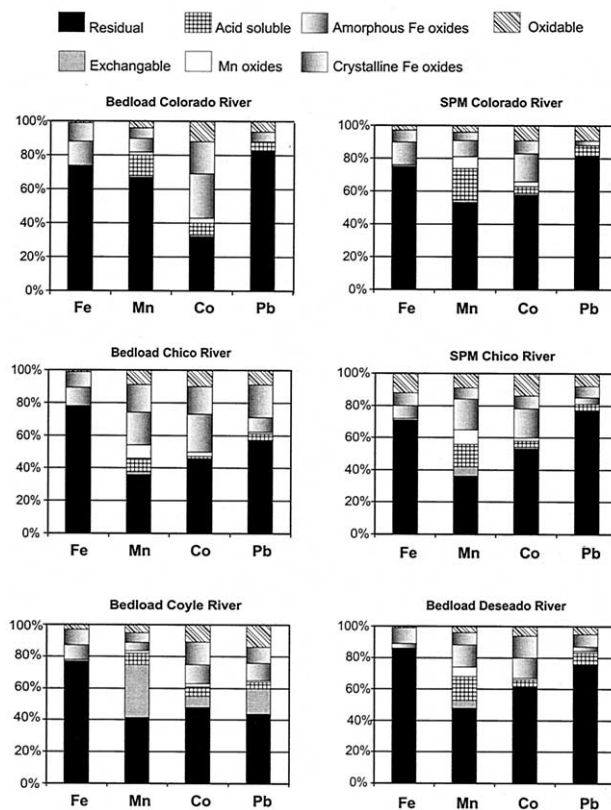

Fig. 4. Trace element distribution among operationally defined fractions of bed sediments, and suspended particulate matter (SPM) of Patagonian rivers.

vironment eventually become associated with bed sediments (Tessier and Campbell, 1987). To examine this phenomenon, we have calculated for each element x, Kd coefficients for the different Patagonian rivers, using dissolved and leachable metal concentrations (extracted with 0.5 N HCl) in bed sediments ($Kd_{diss/leachable} = x_{diss}/x_{leachable}$) (data from Table 5). In agreement with sequential extraction results, Figure 5 also shows the importance of Fe-oxides, and to a lesser extend organic matter, as important phases in the control of metal speciation. Noticeably, Figure 5 suggests a competition for the mobile metals between the dissolved phases and the particulate compounds. Taking Co as an example, a decreasing trend of Kd $Co_{diss/leachable}$ (increased leachable metals in bedload samples) is observed both with increasing leachable Fe from bed sediments (leachable-FeBS) and the percentage of particulate organic carbon (POC) in the suspended matter.

4.2.1.2. Influence of physico-chemical conditions on metal partition: The importance of DOC in Fe control. In waters under circumneutral pH and oxic conditions (as found in Patagonian rivers), Fe is thought to occur primarily in the oxide form, with organic and inorganic complexes enhancing colloidal stability (Stumm and Morgan, 1996). In Patagonian rivers (Fig. 6a), dissolved Fe shows a strong relationship with DOC concentrations probably because dissolved organic matter stabilizes Fe colloids (Boyle et al., 1977; Sholkovitz et al., 1978; Sholkovitz and Copland, 1981; Dai and Martin, 1995; Viers et al., 2000). The solubility of Fe may be enhanced by a strong
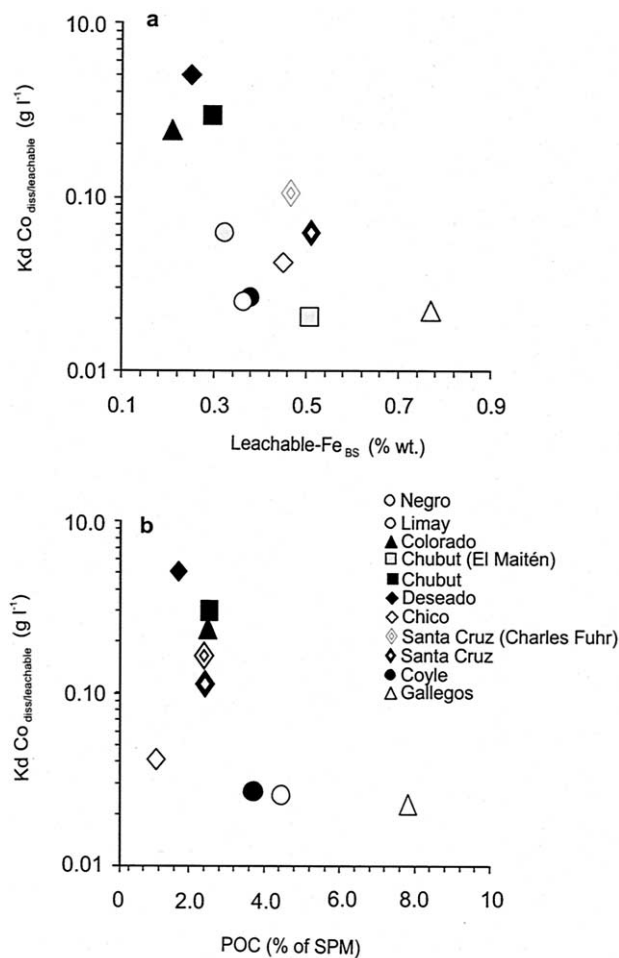
Fig. 5. Plot of trace element partition distribution (Kd Co$_{diss/leachable}$ [in bed sediment] = $x_{diss}/x_{leachable}$) vs. river bed sediment leachable Fe, and the average percentage of particulate organic carbon (POC) for different Patagonian rivers. Similar relationships are observed for Pb, and Cu but not for Ni and Mn.
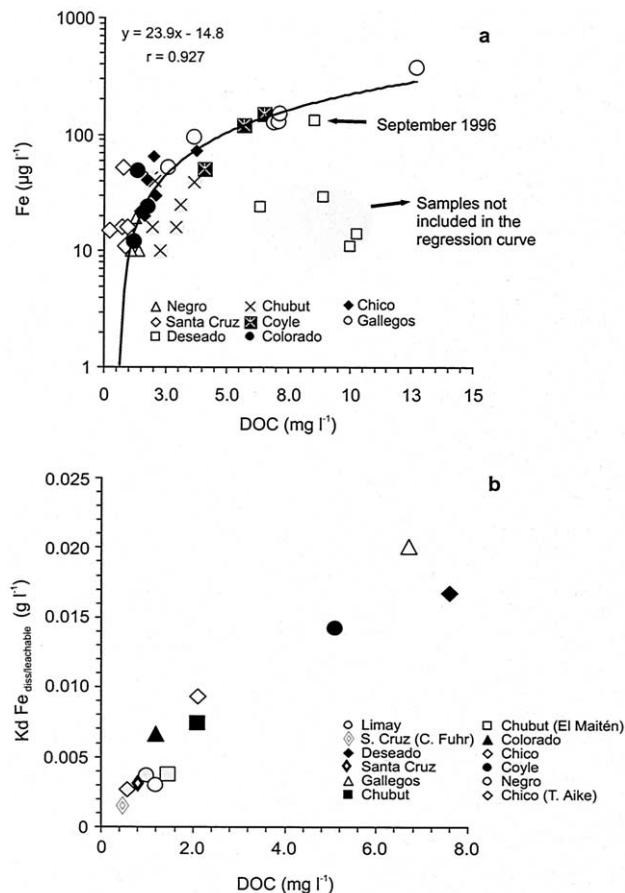
Fig. 6. (a) Relationship between dissolved organic carbon (DOC) and dissolved Fe concentrations. Samples correspond to values obtained in different seasons at lower basin stretches. Only the indicated sample (September 1996 from the Deseado River) is included in the regression curve. (b) Mean DOC concentrations vs. Kd Fe$_{diss/leachable}$. Leachable metals were calculated using values from bed sediments.

complexation with DOC (Fig. 6b), which in turn could inhibit its adsorption as oxides onto riverine particles and thus limiting its metal scavenging power (Salomons and Förstner, 1984). In the particular case of the Gallegos and the Coyle rivers, a relatively minor presence of Fe-oxide particles allows a higher proportion of metals to be transported in the dissolved load (Fig. 2), probably stabilized by organic complexes. In these rivers, organically complexed metals could be adsorbed by POC and eventually fixed onto bottom sediments (Fig. 5). This could explain the depletion of some elements in the suspended load (see Fig. 3f) and, the relatively higher abundance of metals associated with the exchangeable and organic matter fraction of bed sediments (see Coyle River, Fig. 4).

4.2.1.3. The inorganic control of trace elements transport: pH and ionic strength. Iron complexing by DOC appears to be less effective in river waters with high pH, and high ionic strength as is indicated in Figure 6a for the Deseado River. At higher pH, the propensity of trace metals to associate with sediments increases due to precipitation or sorption processes (Tessier et al., 1996). Under such water conditions it is highly

probable that the solubility of Fe would mainly be controlled by inorganic ligands (e.g., $-OH^-$ or CO_3^{2-}) (see Fig. 7) which may eventually decrease its concentration in solution due to precipitation. For the Deseado River, a unique sample that fit well on the curve of Figure 6a may indicate the existence of an effective mechanism of competition between the organic and inorganic ligands. Hence, the complexing of dissolved Fe by DOC seems high at relatively low pH and conductivity, as demonstrated by both variables measured in September 1996. Accordingly, Figure 8 shows that Kd$_{diss/total-SPM}$ values for Cu (also for Pb) seems poorly correlated to total Fe in SPM during September 1996, indicating that the presence of these metals in the particulate fraction is explained by mechanisms other than Fe oxide co-precipitation. Such a situation is most noticeable in those rivers (i.e., Colorado and Deseado) that have both, high pH and high alkalinity. Under these conditions dissolved metal complexation with carbonate ions could be relatively more important for metal speciation when Fe oxides and organic ligands are relatively less abundant. In these rivers, it seems that the transport of metals is highly dependent on water pH, because co-precipitation of complexed dissolved metal will occur only when triggered by carbonate precipitation. The
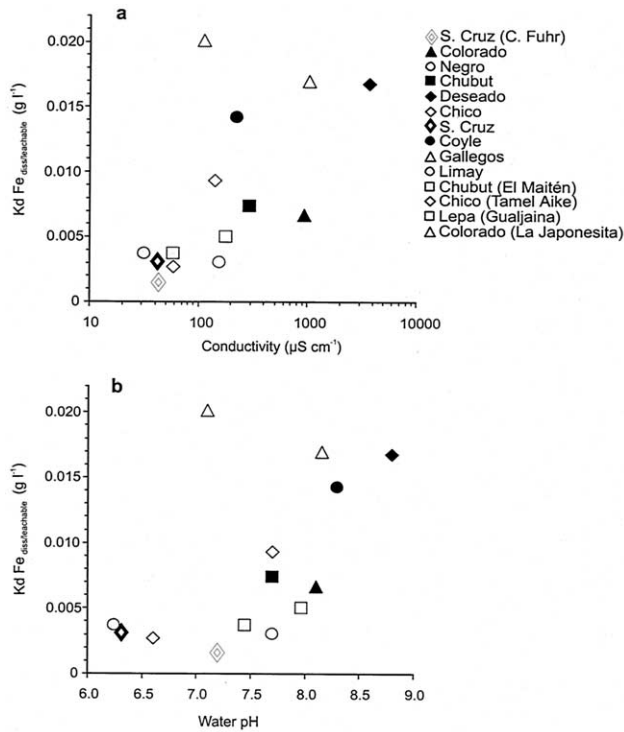
Fig. 7. Plot of conductivity and pH vs. Kd $Fe_{diss/leachable}$ (in bed sediment) $= x_{diss}/x_{leachable}$. For samples taken at the lower basin stretches the values of conductivity and pH are means of different seasonal measurements. Similar relationship is observed for Kd Cu and Pb.

above observations indicate that, in contrast to what is shown by the southernmost rivers (i.e., Gallegos and Coyle), at higher pH and higher ionic strength, inorganic complexes may also enhance trace metals solubility as indicated in Figure 7a. This behavior could explain the transport characteristics of the Deseado and Colorado rivers (Fig. 4).
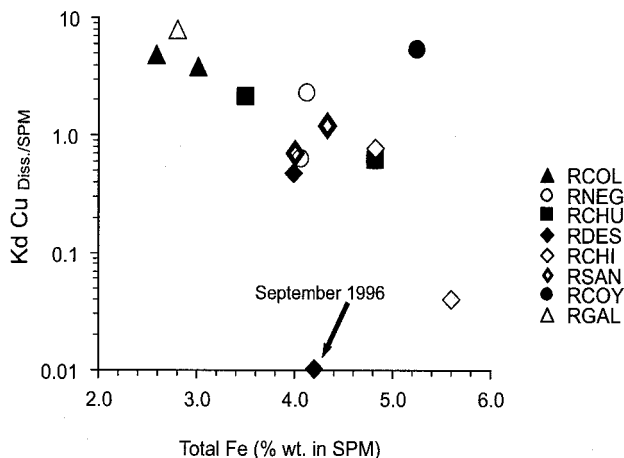
Fig. 8. Plot of Kd $Cu_{diss/SPM} = x_{diss}/x_{SPM}$ vs. total Fe concentration in SPM for different Patagonian rivers. Data correspond to two different sampling periods in each river. Similar relationships are observed for Pb, Ni and Co but not for Mn.
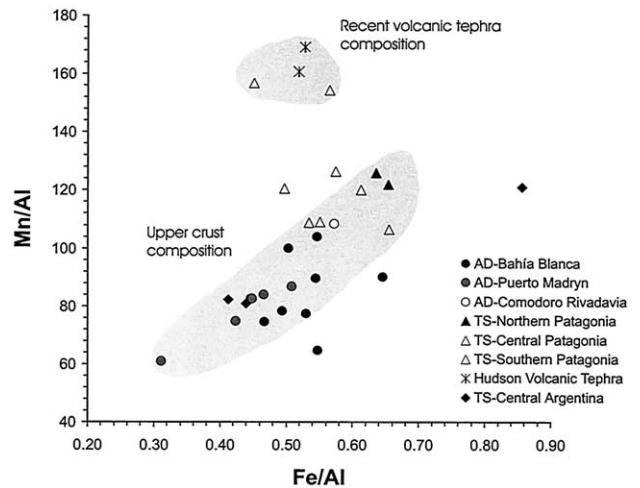
Fig. 9. Relationship between bulk concentrations of Mn vs. Fe, both normalized to total Al in aeolian dust (AD), topsoils (TS) and in two recent Hudson volcano tephra samples. Al and Fe concentration are in wt.% and Mn is expressed in $\mu g \ g^{-1}$.

4.2.1.4. Fe oxides and particle transport dominance. The partitioning of Fe seems to change drastically at low DOC concentrations (Figs. 6a and 6b). Those Patagonian rivers with circumneutral pH waters and lower DOC concentrations and ionic strength, may present a third mode of transport. Under such conditions, trace metals could be predominantly bound to Fe oxides and hence, their transport would be dominated by the particulate fraction (e.g., Santa Cruz, Negro, and Chico, Fig. 2).

Apart from the physico-chemical mechanisms of metals control, it is very important to remark that the final balance between elements transported in solution and in the leachable particulate phases will depend on the total amount of suspended matter carried by the rivers to the ocean. This becomes evident when the characteristics of metal transport by the Chico and Deseado rivers are contrasted with that of rivers having similar chemical characteristics (e.g., compare Chico with Santa Cruz and, Negro with Deseado and with Colorado). The Chico and Deseado rivers have markedly different physico-chemical water characteristics but in both basins land-use has increased the specific yield of particulate metals as a consequence of soil erosion This appears to have favored the subsequent increase of particulate over the dissolved metal transport mode (Gaiero et al., 2002).

4.2.2. Windborne Materials

4.2.2.1. Natural vs. anthropogenic sources of trace elements: The role of topsoils. In Figure 9 Al is used to normalize particulate elemental concentrations to minimize effects of grain-size variation (e.g., Huang et al., 1992) and to clarify association patterns among different elements present in topsoils and aeolian dust samples. The majority of topsoils and aeolian dust samples plot within a shadowed area (Fig. 9), which represent an observed slope of Mn/Fe of 183 ($r = 0.88$; $p < 0.05$) and is close to a similar ratio (171) found in the earth's crust (Taylor and McLennan, 1985). This would suggest that together with Al, the source of Fe and Mn in aeolian dust samples is primarily natural weathered material. Probably, the
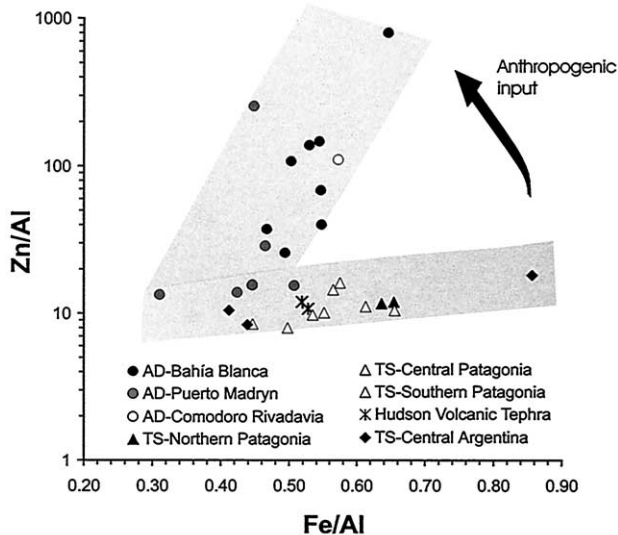
Fig. 10. Relationship between the bulk concentrations of Zn vs. Fe both normalized to total Al in aeolian dust (AD), topsoils (TS) and in two recent Hudson volcano tephra samples. Al and Fe concentration are in wt.% and Zn is expressed in $\mu g \ g^{-1}$. See text for additional explanation.
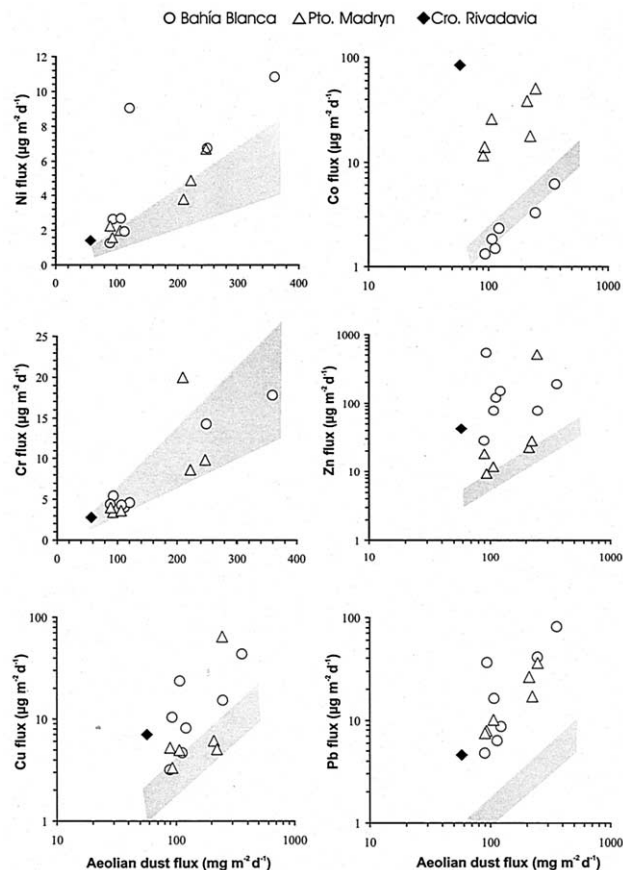

Fig. 11. Plots of aeolian dust fluxes vs. trace elements fluxes for different seasons at the Bahía Blanca, Puerto Madryn, and Comodoro Rivadavia sites. The shadowed areas represent simulated fluxes assuming topsoil compositions. This is done replacing in fluxes calculations real aeolian dust values by their corresponding topsoil concentration (± 1 standard deviation).

Earth's crust composition of some topsoil samples (e.g., the southern ones) is locally modified as a consequence of the fallout of Hudson's Mn-rich 1991 pyroclastic material. On the contrary, some of the aeolian dust samples collected at Bahía Blanca are characterized by a low Mn/Fe ratio (140), which we interpret as indicating a seasonal variation of the sources of dust, probably supplied from areas with topsoils richer in Fe as could be the case of samples from the Argentine Pampa (e.g., topsoil sample from Vicuña Mackenna).

High Zn concentrations are frequently considered as indicators of anthropogenic pollution (Chester et al., 1984). As it is shown in Figure 10, some dust metals (using Zn as an example), do not appear to have a unique source and a seasonal anthropogenic origin may be evident. In the same Figure 10, the volcanic tephra data (see also Table 4 for other elements) suggest that (at least during the studied period) recent volcanic activity is not an important contributor to trace metals in aeolian dust.

Since soils are potential sources of transition metals to the aeolian dust, we estimated a range of aeolian dust fluxes using measured Patagonian topsoils composition. This approach is well supported since the analyzed trace elements in topsoil samples mostly belong to the fine size-fraction (readily picked-up by winds) with a clear regional upper-crustal composition (see Fig. 3). The relationships between trace element fluxes and the total aeolian dust deposition are shown in Figure 11 where the shadowed areas represent simulated fluxes assuming topsoil compositions. This is done by replacing the real aeolian dust values by their corresponding topsoil concentration ($\pm$ one standard deviation). The relationships between trace element fluxes and the total aeolian dust deposition (Fig. 11) could indicate the existence of both, natural and anthropogenic sources particularly for Co, Zn, Cu, and Pb, which probably are linked to the atmospheric transport patterns in the region. Similarly to Al, Fe, and Mn, most of Cr and, to a lesser extent, Ni fluxes appear to be supplied mainly by regional upper-crustal particles (Fig. 11) as it is also suggested by a similar percentage of leachable metals in Table 5. For the northernmost aeolian dust samples (Bahía Blanca), the Co sources seem totally linked to resuspended material from soils, in contrast to the samples from Puerto Madryn and the only composite sample from Comodoro Rivadavia. The latter seems to have an anthropogenic origin for Co restricted to the Patagonia region. The central part of Patagonia is known by its important oil industry and Co is released to the environment from the burning of fossil fuels (Liennemann et al., 1997). A acid-extracted analysis of a sample from Puerto Madryn indicates that ~90% of Co is transported in the mobile fraction of the aeolian dust (Table 5), unlike results for Bahía Blanca aeolian dust and for topsoils samples.

The group of aeolian dust samples shows that measured Pb fallouts are always higher than the fluxes estimated from topsoils, having a noticeable relationship with increased aeolian dust deposition ($r = 0.86$; $p < 0.05$). This is not unexpected since the extended usage of leaded gasoline presents a persistent local and regional source in time. This is further supported
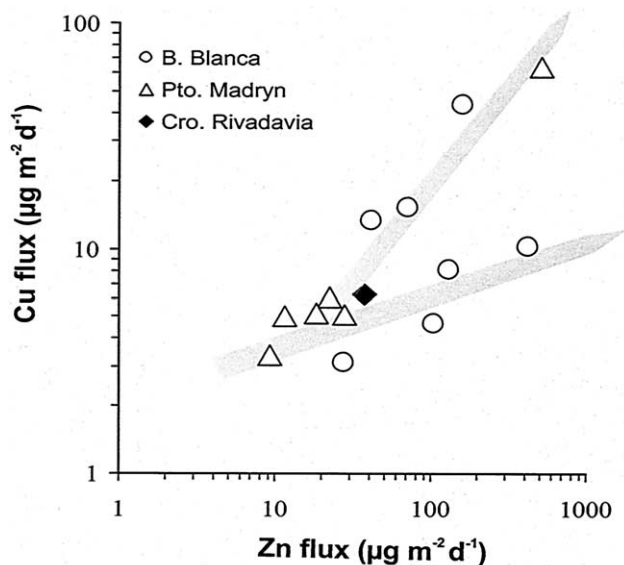
Fig. 12. Plot of Zn fluxes vs. Cu fluxes for different seasons at the Bahía Blanca, Puerto Madryn, and Comodoro Rivadavia sites.
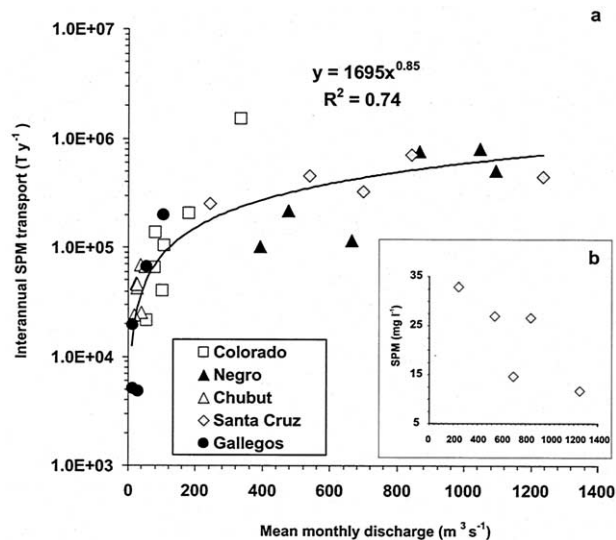

Fig. 13. (a) Relationship between mean monthly discharge and the interannual suspended load (SPM) transport for different Patagonian rivers. Correlation is significant at $p < 0.05\%$ level. (b) In the Santa Cruz River, the presence of pro-glacial lakes at the foothills of the Andes acts as sediment traps for most of the sediment produced at the higher catchments and determine that at higher discharges, SPM concentrations are lower (dilution), maintaining the maximum sediment transport below 1.0×10^6 T yr^{-1}.

by the higher concentration of mobile Pb in the aeolian dust samples (Table 5). In contrast, the relationship between the total aeolian dust vs. Cu and Zn fluxes indicates episodic local or regional pollution, combined with periods of non polluted Earth's crust material deposition. The source of both elements seems highly dependent on climatic conditions. The relationship between their fluxes (Fig. 12) suggests a common source, probably linked to anthropogenic emissions from the Chilean mine El Teniente (34°S) through its huge associated Caletones smelter, which is the major source of contamination with S, Cu, Zn, and As in the region (Romo-Kröger et al., 1994). Wolff et al. (1999), attributed high Cu concentrations in Antarctic snow to emissions from the above mentioned area. In Figure 12, the change in the slope of some Bahía Blanca samples indicates an increase of Zn over the Cu flux which could be explained by the particles not being directly associated with smelting activities but perhaps to coarse material processed in the mine (Romo-Kröger et al., 1994).

4.3. Transition Metals Transfer From Patagonia

4.3.1. The Riverine Path

4.3.1.1. Sediment Transfer. Patagonian rivers deliver peak water influxes to the coastal zone during the late southern summer-early fall (rainfall during February–April) and at the beginning of the spring (snowmelt, September–October). The total riverine water discharge is ~1700 m^3 s^{-1}. The Negro and Santa Cruz rivers are the main water suppliers (46 and 42% respectively of the total Patagonian discharge), with the remaining rivers accounting for the rest.

In agreement with data from the largest world rivers (Trefry and Presley, 1976; Gibbs, 1977; Yeats and Bewers, 1982; Dupré et al., 1996), most of the trace elements in Patagonian rivers are mainly transported in the SPM fraction (Gaiero et al., 2002). Using an empirical relationship between river sediment yields and a large number of hydroclimatic, biologic, and

geomorphological parameters, Ludwig and Probst (1998) estimated for the northern and southern Patagonian coastal regions, total river sediment inputs of 5 to 50×10^6 and <0.5 to 10×10^6 T yr^{-1}, respectively. Based on the minimum and the maximum suspended load transported by each river, we can estimate that the entire region exports, via the riverine path, between 0.5×10^6 and 4.3×10^6 T yr^{-1} (mean of 2.0×10^6 T yr^{-1}) of SPM to the South Atlantic Ocean, which represents only ~2% of the total annual export by the Río de la Plata (McLennan, 1995).

Figure 13 summarizes the relationship between mean monthly discharge and the interannual SPM transport for those Patagonian rivers with known discharge. This figure shows that the two northernmost Patagonian rivers supply ~40% of the load, and the Santa Cruz River additionally contributes with 25% of the total SPM delivered to the ocean. In spite of the large seasonal variability in discharge (Fig. 13), the largest rivers show the most regular interannual sediment transport (Negro, $0.10-0.80 \times 10^6$ and Santa Cruz, $0.25-0.75 \times 10^6$ T yr^{-1}). For the Santa Cruz river (and to a lesser extend the Negro river), higher discharge correlates with lower SPM. This is probably due to the trapping effect of the Argentino and Viedma lakes.

Storms that take place downstream from dams and lakes and induce flood events can be significant contributors to the sediment budget. During April 1998 we witnessed heavy rainfall events that flooded the lower Chubut River valley (rainfall was 250 mm in 4 d in an area where the mean annual precipitation is 150 mm). The flood event lasted ~7 d and we estimate that the discharge for this period was twice (80–100 m^3 s^{-1}) as much the mean monthly value. Using a mean SPM concentration of 730 mg L^{-1} (measured the 6th day of the flood event)
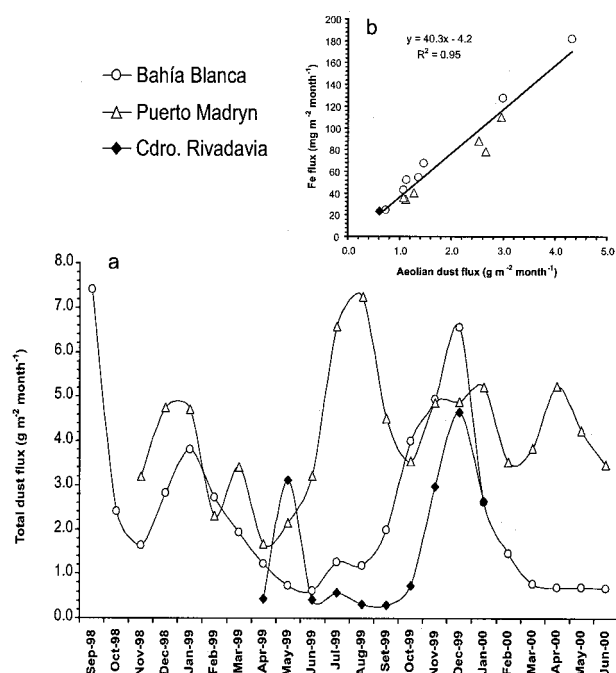
Fig. 14. (a) Seasonal dust fluxes measured at three different sampling stations along Patagonia's coast. (b) Relationship between total dust deposition and total Fe deposition for samples from the three stations as in (a). Replacing the total dust flux from a) on the x in the equation of (b), allows the estimation of the windborne Fe reaching the nearby ocean during the sampling period.

the estimated transfer of sediment was 0.035×10^6 T, which is ~75% of the total mean interannual export of this river.

Although locally significant, this type of flooding represents only 2% of the mean interannual exported by all Patagonian rivers. Such heavy rainfall events that increase transfer of sediment to the coastal zone are exceptional. The water source for Patagonian rivers is the narrow area along the Andes, which in turn becomes the only source of weathered material transported to the ocean. Despite the large sediment yields on the Andes (modeling suggests $100–1000$ g m^{-2} yr^{-1}, Ludwig and Probst, 1998), a significant proportion of the particulate load carried by the largest rivers is retained in pro-glacial lakes (e.g., Limay River—a tributary of the Negro—and, Santa Cruz River) or reservoirs (e.g., in the Negro, Colorado and Chubut rivers) before entering the coastal zone. This situation promotes a low sediment yields for the region (7.0 g m^{-2} yr^{-1}) which is 25 times lower than the estimated for South America (McLennan, 1995) and is comparable to yields modeled in world desert areas by Ludwig and Probst (1998).

4.3.2. The Aeolian Path

4.3.2.1. Aeolian dust fallout. Patagonian dust fallout data indicate that the total dust fluxes are highly variable with marked seasonal patterns ranging from 0.3 to 8.1 g m^{-2} month^{-1} over the total sampling period (mean of 35 g m^{-2} yr^{-1}). The highest fluxes were measured at Puerto Madryn with a range of 1.9 to 8.1 g m^{-2} month^{-1} and a yearly mean of 55 g m^{-2}. The Bahía Blanca dust flux ranged from 0.4 to 7.4 g m^{-2} month^{-1}, with a yearly mean of 26 g m^{-2}. Fluxes during the

sampling period were lower at Comodoro Rivadavia, ranging from 0.3 to 4.7 g m^{-2} month^{-1} with a yearly mean of 19 g m^{-2}. The three records show different seasonal patterns (Fig. 14). At Bahía Blanca, it shows three peaks, in September 1998 (early spring), January and December 1999 (summer) and the lowest values were recorded during April-August (autumn-early winter). At Puerto Madryn the highest fallout flux peak are in February 1999 (summer), June 1999 (winter) and September 1999 (early spring), followed by minor peaks on summer and the beginning of autumn. At Comodoro Rivadavia, the record shows two fallout peaks, in autumn and summer.

In spite of different dust sampling devices, our Patagonian dust fluxes estimates are similar to that measured by Ramsperger et al. (1998) (i.e., $0.6–11$ g m^{-2} month^{-1}) in the NE Patagonia region (Bahía Blanca and surroundings). Also, Patagonian mean dust deposition is similar to that found for the eastern Mediterranean Sea, but higher than the mean deposition rate (18 g m^{-2} yr^{-1}) for the entire sea (Guerzoni et al., 2001).

Prospero et al. (2002) employed the TOMS sensor to map the global distribution of major atmospheric dust sources. Their study showed that Patagonia, along with western Argentina and Bolivia's Altiplano are South America's most persistent dust sources. These remotely-identified sources are coherent with the results supplied by models. Tegen and Fung (1994) developed a global three-dimensional model of the atmospheric mineral dust cycle, based on the distribution of vegetation, soil texture, and soil moisture. Their modeled output of the total annual dust deposition rate for Patagonia and for a sector of the adjacent Argentine shelf is between 10 and 100 g m^{-2}. Further out to sea, the model predicts deposition rates in the order of 1 to 10 g m^{-2} yr^{-1}. The GOCART model (Ginoux et al., 2001) also identifies the Patagonian plateau as a significant dust emission area. The annual deposition rate predicted by this model is somewhat lower than the results published by Tegen and Fung (1994): 5 to 10 g m^{-2} yr^{-1} on the land and 1 to 5 g m^{-2} yr^{-1} on the shelf. The total GOCART-simulated deposition for the south Atlantic is 20 Tg yr^{-1}, which is close to the mass (24 Tg yr^{-1}) estimated by Duce et al. (1991). Therefore, data gathered through direct sampling appears to agree better with the model of Tegen and Fung (1994) than with the GOCART model.

4.3.2.2. Transport. Dust deposition, which is significant along the Patagonian coastline, could be important to the South Atlantic Ocean. Textural analyses with SEM on a set of aeolian dust samples of Bahía Blanca show a mean particle size between 5 and 20 μm (Bidart, in preparation). The lifetime of small silt ($1–10$ μm) in the atmosphere is on the order of days (Tegen and Fung, 1994) and Sedigraph's analyses of aeolian dust samples from the three sampling stations indicate that a mean of 86 ± 4% of the mass correspond to particles with diameters < 10 μm. Atmospheric circulation and transport of particles from Patagonia are observed in satellite images of the ash plume extending ESE from the Hudson volcano during the 1991 eruption (Fig. 15a, taken from: http://www.volcano.si. edu/gvp/volcano/region15/andes_s/hudson/var.htm). Clouds of fine volcanic ash and sulfur dioxide gas from Hudson's 1991 circled the South Polar Region nearly three times before dispersing (Constantine et al., 2000). Also, satellite images revealed that 2 months after to the paroxysmal eruption, a volcanic plume from the vicinity of the volcano (surely uplifted by
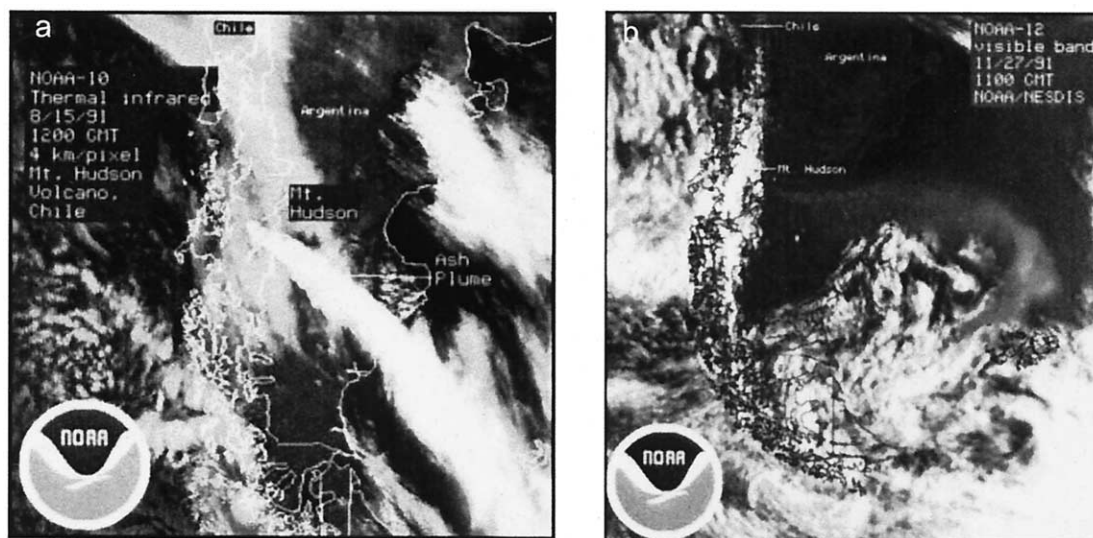
Fig. 15. Satellite images serve as an indirect tool to show the importance of atmospheric circulation and transport of particles from Patagonia. (a) Infrared image from the NOAA 10 polar-orbiting weather satellite on August 15, 1991, showing the ash plume extending SE from the Hudson volcano. (b) Visible-band image from the NOAA-12 polar-orbiting weather satellite on November 27, 1991, showing an ash plume extending from the vicinity of the Hudson volcano to the western Atlantic Ocean 3 months after the main eruption event. Both images were taken from: http://www.volcano.si.edu/gvp/volcano/region15/andes_s/hudson/var.htm.

strong winds) extended > 1000 km across southern Argentina and the western Atlantic Ocean (Fig. 15b, taken from the same source as Fig. 15a) (Global Volcanism Network Bulletin, 1991). Tephra from the 1991 eruption was detected on the ground on Malvinas (Falkland) Island (several centimeters of accumulation) and on South Georgia (>2700 km from Cerro Hudson) $\sim$2 weeks after the main eruption (Smellie, 1999). Also this author mentions that atmospheric turbidity was observed over two widely separated Antarctic stations.

From August 12 to 15, 1991, it was estimated that on the Patagonia Argentinean side $\sim$23 $\times$ 10^6 T of tephra was deposited on an area of 100,000 km^2 (Scasso et al., 1994) giving a daily deposition rate of 5800 g m^{-2}. Contrary to normal isopach patterns, maximal depositions were found 500 km from the volcano, close to the Atlantic coast. Beginning August 16 and lasting for 1 week, strong westerlies swept the deposited tephra off to the ocean (Scasso et al., 1994).

4.3.3. Total Trace Element Fluxes to the South Atlantic Ocean

Tegen and Fung's (1994) global model of dust deposition showed comparable total annual dust deposition at the Patagonian coast and, over an area of the ocean approximately similar to that of the Patagonian Argentine shelf (i.e., 0.83 $\times$ 10^6 km^2). Using the mean dust deposition measured by us at the Patagonian coastline (i.e., 35 g m^{-2} yr^{-1}) over this shelf area, we estimate that the shelf receives a dust input of 29 $\times$ 10^6 T yr^{-1}. The mean riverine input to the coastal zone accounts for a much smaller annual input of $\sim$2.0 $\times$ 10^6 T yr^{-1}. Since the model of Tegen and Fung (1994) successfully describes the seasonality and deposition rates of mineral dust at the few locations where such observations have been made, there is reason for confidence in extending the above calculation to the entire shelf area.

An additional important source of material to the shelf originates from coastal erosion of about half (1600 km) of the Patagonian coastline that is made up by cliffs composed of relatively unconsolidated Eocene and Miocene sediments (Pierce and Siegel, 1979; Schnack, 1985). Pierce and Siegel (1979) estimated that 39 $\times$ 10^6 T yr^{-1} of sediment are supplied to the shelf by cliff erosion of the southern (385 km) coastline. This estimation is a matter of debate as the mentioned authors based their calculation on the very high cliff erosion rate of 1 m yr^{-1}. This figure can be considered as an upper limit to be a maximum input for the whole shelf. Thus we assign an estimated total supply of Patagonian terrigenous sediments to the shelf of 70 $\times$ 10^6 T yr^{-1}.

The Argentine shelf is composed primarily of sandy or coarse sediments (Urien and Ewing, 1974), which could indicate that most of the fine particles delivered through rivers, winds, and cliff erosion are removed from the shelf. This export is believed to be a significant contribution to the nepheloid layer and to the bottom sediments of the Argentine Basin (Pierce and Siegel, 1979), where the mean deposition rate is estimated on 30 g m^{-2} yr^{-1} (Ewing et al., 1971), representing a total input of 30 $\times$ 10^6 T yr^{-1} (Ewing et al., 1971; Biscaye and Eittreim, 1977). Based on our budget and considering also a substantial input of sediments from the Río de la Plata to the Argentine Basin (Klaus and Ledbetter, 1988), a significant mass of Patagonian sediments may be transported out of the area by oceanic currents. Hydrographic processes are thought to transport fine-grained minerals from the Argentinean shelf to the northern Scotia Sea (Diekmann et al., 2000; Walter et al., 2000) where smectite and quartz rich sediments are consistent with a Patagonian source (Pierce and Siegel, 1979; Gaiero et al., 2002). As indicated by the model of Tegen and Fung (1994), direct Patagonian dust input to the open South Atlantic
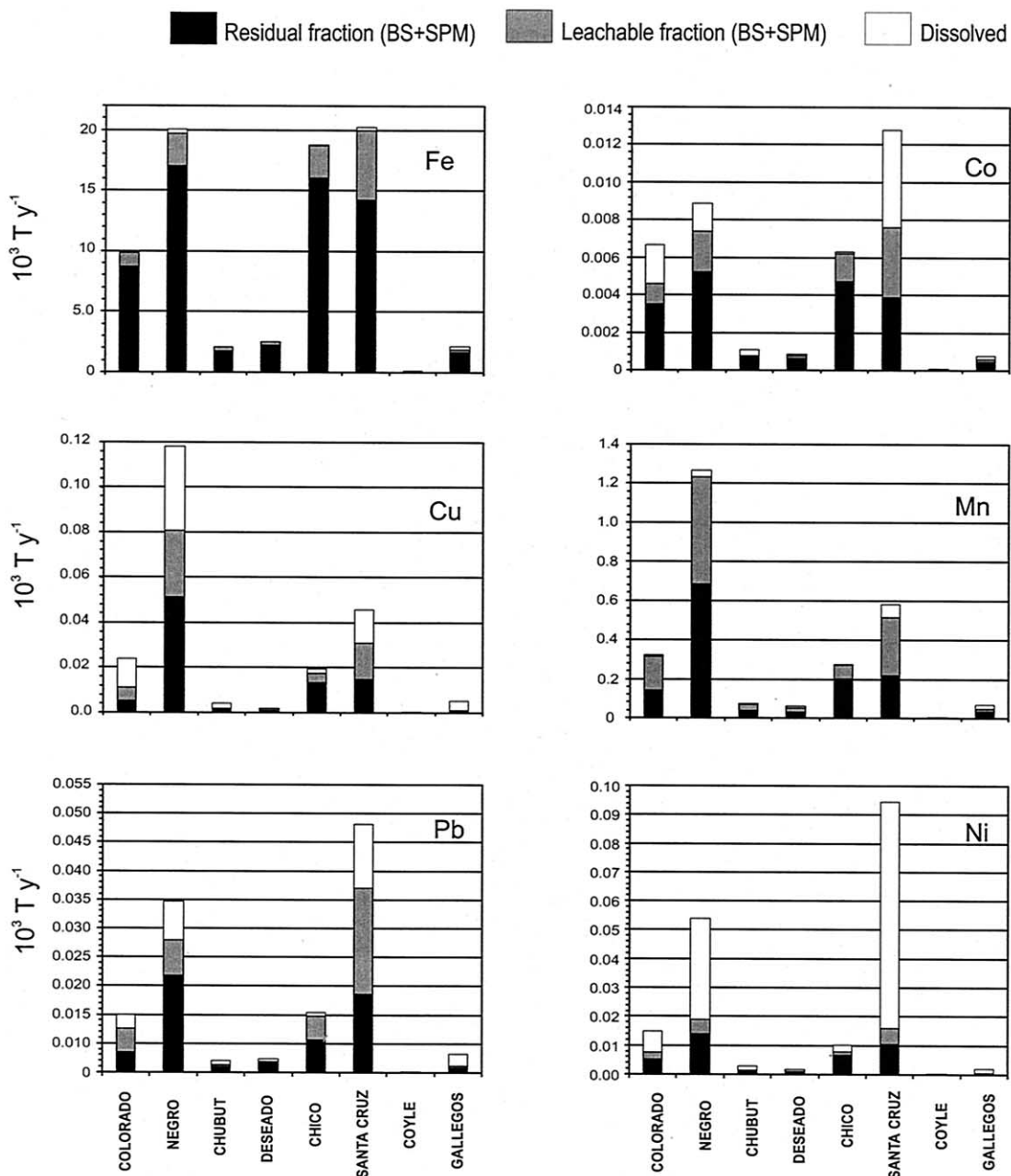
Fig. 16. Total trace elements transported by the different Patagonian rivers to the southern South Atlantic coastal zone. Different shades on the bars indicate the relative proportion of trace elements transported by particles (BS-bed sediments + SPM-suspended particulate matter) on both, the residual (black) and leachable (gray) fractions. The white part of the bars indicates the relative proportion transported in the dissolved fraction.

Ocean may be significant. Furthermore, signatures of magnetic susceptibility in sediment cores of the Scotia Sea are similar to the dust record of the Vostok ice core most likely derived from titanomagnetite-rich Patagonian dust (Hoffmann, 1999).

4.3.3.1. Riverine trace element inputs. Figure 16 shows the fractions transporting trace elements in Patagonian rivers. The leachable fraction and the dissolved load are the most important in terms of micronutrients supplied to marine organisms of the Patagonian shelf water. The two largest rivers, Santa Cruz and Negro, account for ~70% of the total riverine trace metals

exported from Patagonia. Since the Santa Cruz River is scarcely affected by human activity, its characteristics may be useful for reconstructing preindustrial transport conditions in high latitude environments.

Figure 16 shows that significant amounts of the metals reach the Patagonian coast in the dissolved load (e.g., Cu, Pb, Ni, and Co). However, it must be stressed that estuarine processes drastically modify the riverine composition and ultimately control inputs to the ocean. Patagonian estuaries are very diverse (Piccolo and Perillo, 1999). Their chemical, biologic, geolog-

Table 6. Mean values and one standard deviation for aeolian trace element fluxes at the Patagonian coast. All data in the first three columns expressed in $\mu g\ m^{-2}\ d^{-1}$ except for Al and Fe (*) expressed in $mg\ m^{-2}\ d^{-1}$.

	Aeolian dust B. Blanca	Aeolian dust P. Madryn	Estimated from topsoil	Hudson volcanic tephra $(10^3\ mg\ m^{-2})$[a] 4 d total
Al*	12.5 ± 8.4	12.8 ± 6.8	11.6 ± 6.6	2,020
Fe*	6.6 ± 4.6	5.4 ± 2.7	6.6 ± 3.8	1,040
Mn	104 ± 86	98 ± 49	137 ± 78	8.1
Ni	4.9 ± 4.0	3.5 ± 2.0	2.6 ± 1.5	0.07
Co	2.4 ± 1.9	26 ± 15	3.1 ± 1.8	0.40
Cr	7.5 ± 5.9	8.3 ± 6.4	7.9 ± 4.5	0.11
Zn	164 ± 174	102 ± 200	13 ± 7.6	2.2
Cu	14 ± 14	15 ± 24	4.8 ± 2.7	nd
Pb	27 ± 28	18 ± 12	2.4 ± 1.4	0.32

[a] Based on HVT-1 values from Table 4.

nd = not detected.

ical, and physical compositions must be fully understood to accurately determine chemical fluxes and thus refine the geochemical mass balance of this region.

4.3.3.2. Aeolian dust trace element inputs. Using topsoils transition metals compositions, we estimated aeolian dust fluxes (Table 6). The chemical composition of the Hudson volcanic tephra obtained shortly after deposition at Puerto San Julián (see Table 4), was used to estimate the total trace elemental deposition during the short event of August 12 to 15, 1991 (Table 6). Table 6, also compares the mean daily flux of trace elements estimated for Bahía Blanca and Puerto Madryn. These fluxes are of the same order of magnitude to trace element dry deposition measured over the Ligurian Sea (Migon et al., 1997).

Aeolian input of the transition metals over the Argentine shelf is several times higher than the one delivered by rivers (Table 7). Except for Pb and Cu, this finding contrasts with the situation for the Mediterranean Sea, where most of the trace elements are mainly supplied by rivers (Guerzoni et al., 2001).

The fluxes of leachable Cu, Co, and, Pb are comparable in aeolian and riverine material but leachable Fe, Mn and, Ni fluxes are higher in riverine material. Leachable Cu, Co, and,

Pb in aeolian dust samples are more concentrated than in topsoils. Moreover, the percent labile fraction measured in the aeolian dust should be considered as a lower limit since the readily soluble metals may have been washed-out during our aeolian dust treatment.

4.3.3.3. The iron case-study. The main contributors of Patagonian riverine Fe are the Negro, Chico and Santa Cruz rivers (Fig. 16). The total annual riverine Fe load is estimated to be 27 to 165×10^3 T. Riverine suspended sediments can contribute with 4.0 to 26×10^3 T yr^{-1} of Fe present in the leachable fraction, whereas 0.24 to 2.9×10^3 T yr^{-1} reaches the Patagonian estuaries in the dissolved form. However, iron supplied by Patagonian rivers is likely a minor fraction of the aeolian contribution (Table 7).

We estimate a total annual Fe deposition to the coastal zone of 900 to 4400 mg m^{-2} (mean of 2200 mg m^{-2} yr^{-1}) 9% of which is present in the leachable form. This range is in agreement with the Fe deposition (1100–4470 mg m^{-2} yr^{-1}) modeled by Fung et al. (2000) for the Patagonian coast, and is among the highest coastal deposition rates in the world. This result is about five times higher than the rate for the Mediterranean Sea (Guerzoni et al., 2001). Although acid attack does

Table 7. Estimated total riverine (TRF), aeolian (AF), and soil-based aeolian (SAF) trace element fluxes ($x10^3$ T y^{-1}) to the South Atlantic Ocean.

	TRF Total	TRF % LF[b]	AF[a] Total	AF[a] % LF[b]	SAF[a] Total	SAF[a] % LF[b]	AF/TRF	AF/SAF
Fe	86	17	1950	9	2140	2	23	0.9
Mn	2.9	48	33	24	44	18	11	0.8
Co	0.04	50	4.6	40	1.0	15	115	5
Ni	0.2	67	1.4	20	0.9	18	7	2
Pb	0.1	50	7.3	55	0.9	21	73	9
Cu	0.2	55	4.7	45	1.5	14	24	3
Zn	0.5	na	43	na	4.3	na	86	10
Cr	0.3	na	2.6	na	2.6	na	9	1

TRF = Grand total of mean interannual fluxes for all Patagonian rivers, all phases considered (i.e., SPM + bedload + dissolved).

[a] The annual transport for aeolian dust and soil-based aeolian fluxes was estimated for the Argentinean shelf area. See discussion in section 4.3.3. AF = estimated from the mean deposition measured at B. Blanca and P. Madryn (see Table 6).

SAF = estimated from mean data (Table 6).

[b] LF = Leachable fraction (0.5 N HCl); %LF represents the mean percentage of leachable metals (Table 5) in aeolian dust (AF) and topsoil samples (SAF).

na = not analyzed.

not necessary mimic reactions at the seawater surface, 9% of Fe can be viewed as the upper limit of the extractable Fe concentration entering the ocean. This amount is consistent with the 10% of soluble Fe used by Duce and Tindale (1991), and Fung et al. (2000) in their estimation of available Fe supplied via aeolian deposition to the World ocean.

Table 6, shows that only for the 4 d of 1991 Hudson's volcanic eruption, the estimated total trace element deposition was several thousand fold higher than that deposited yearly by the atmospheric Patagonian dust fallout. The August 12 to 15 Hudson's Fe deposition is equivalent to ~500 yr of Patagonian Fe dust fallout. Leachable Fe represent ~3.0% of the total concentration on the tephra sample from Puerto San Julián (Table 5) (while leachable Al = 0.9% and Si = 0.3%). Supposing that only 10% of the ash reached the open ocean and, 1% of it were soluble, then a minimum of ~1000 mg m^{-2} of leachable Fe was introduced in some areas of the Southern Ocean during 1991 Hudson's eruption. The Hudson volcano has been active throughout the Holocene with at least 12 explosive eruptions including that of August 1991 (Naranjo and Stern, 1998).

5. CONCLUSIONS

In contrast to the global budget for which rivers dominate, Patagonian sediments (not considering cliff erosion) are transferred more effectively through the atmosphere to the South Atlantic Ocean. The bulk of particle-borne transition metals transported by Patagonian rivers show a dominant upper crustal composition. The transport of mobile trace elements through the riverine path has shown different patterns linked to the geochemical behavior particular to each element and to the physico-chemical conditions governing each Patagonian river. Particulate leachable trace metal concentrations are mainly controlled by Fe-oxides. Our data reinforce the idea of competition between the organic and the inorganic phases controlling metal speciation and partitioning in aquatic systems. The partitioning of Fe by DOC appears as a key mechanism determining the phases transporting trace metals in Patagonian rivers:

1. in rivers with low ionic strength and relatively higher DOC concentration, trace elements are mainly associated with the dissolved load, probably as a consequence of metal complexation by the organic matter and inhibition of Fe-oxide formation thus preventing metal co-precipitation;
2. in river waters with relatively high ionic strengths, dissolved inorganic ligands are more effective complexing trace metals and their partitioning is more dependant on water pH conditions;
3. in rivers with the lowest suspended load concentrations, and low ionic strength and DOC concentrations, metals are thought to be predominantly bound to Fe-oxides and hence, the transport is dominated by the leachable particulate fraction.

The strikingly low metal fluxes exported by Patagonian rivers, when compared with the aeolian flux, is directly linked to their low suspended particulate load. Most of the riverine particles are thought to be retained in lakes or in reservoirs, determining that many trace elements in some rivers are mostly transported in the dissolved load. More than 90% of the total annual riverine Fe load is delivered by the SPM fraction. Considering a scenario without pro-glacial lakes during the preglacial period and based on the model of Ludwig and Probst (1998) for Andean sediment yield, it is possible to estimate sediment export to the South Atlantic Ocean ~50 times higher than today's estimate for Patagonian rivers. This could have important paleoenviromental implications in the preglacial South Atlantic Ocean, which probably received a higher load of iron than today, thus enhancing the local ocean productivity.

In contrast to the riverine transport path, trace elements determined in aeolian materials have a combined crustal and anthropogenic origin. In general, the aeolian materials reaching the Patagonian coast have transition metals compositions similar to that found in regional topsoils. Seasonal concentrations of some metals however, are much higher than what would be expected from normal crustal weathering, thus implicating pollutant scavenging by wind-transported soil particles. The chemical composition of aeolian dust samples is not matched in Patagonian riverine materials. Due to westerly dynamics, atmospheric dust is not effectively deposited inland but rather blown directly to oceanic waters.

Based on our Fe deposition measurements at the Patagonian coastline, and supposing that ~1% of the measured coastal flux reaches the open ocean, the sub Antarctic South Atlantic (a HNLC area) could receive between 1.0 and 4.0 mg m^{-2} yr^{-1} of leachable Fe. Such flux range probably represents minimum deposition rates. Modeling efforts will undoubtedly contribute to the better understanding of the mechanisms controlling the transport of Patagonian dust to the open ocean.

Indeed, not considering coastal erosion we estimate that ~250 mg m^{-2} yr^{-1} of leachable Fe can eventually reach the nearby South Atlantic Ocean primarily via the atmospheric pathway. Moreover, evidence suggests that trace elements delivered to the Patagonian shelf by cliff erosion, and the riverine and the aeolian paths could occasionally reach the open ocean by hydrological transport.

In this paper we note the importance of past (late Holocene) and present volcanic activity delivering particles to the ocean. It must be stressed that each of such events can contribute leachable Fe to the ocean several thousands fold the mass introduced by annual dust fallout. Is such Fe readily available for primary production? If it is, it could have triggered an important phytoplankton bloom on the HNLC areas of the South Atlantic Ocean and Southern Ocean during the austral summer of 1991 to 1992.

Associate editor: K. K. Falkner

REFERENCES

Agemian H. and Chau A. S. Y. (1976) Evaluation of extraction techniques for the determination of metals in aquatic sediments. *Analyst* **101**, 761–767.

Barnola J. M., Raynaud D., Korotkevich Y. S., and Lorius C. (1987) Vostok ice cores provides 160,000-year record of atmospheric CO_2. *Nature* **329**, 408–414.

Basile I., Grousset F. E., Revel M., Petit J. R., Biscaye P. E., and Barkov N. I. (1997) Patagonian origin of glacial dust deposited in East Antarctica (Vostok and Dome C) during glacial stages 2, 4 and 6. *Earth Planet. Sci. Lett.* **146**, 573–589.

Bendell-Young L. and Harvey H. H. (1992) The relative importance of manganese and iron oxides and organic matter in the sorption of trace metals by surficial lake sediments. *Geochim. Cosmochim. Acta* **56**, 1175–1186.

Biscaye P. E. and Eittreim S. L. (1977) Suspended particulate loads and transports in the nepheloid layer of the abyssal Atlantic Ocean. *Mar. Geol.* **23**, 155–172.

Boyle E. A., Edmond J. M., and Sholkovitz E. R. (1977) Mechanism of iron removal in estuaries. *Geochim. Cosmochim. Acta* **41**, 1313–1324.

Chester T., Sharples E. J., Sanders G. S., and Saydam A. C. (1984) Saharan dust incursion over the Thyrrenian Sea. *Atmos. Environ.* **18**, 929–935.

Clapperton C. (1993) *Quaternary Geology and Geomorphology of South America.* Elsevier, Amsterdam, the Netherlands.

Constantine E. K., Bluth G. J., and Rose W. I. (2000) TOMS and AVHRR observations of drifting volcanic clouds from the August 1991 eruptions of Cerro Hudson. *Geophys. Monogr.* **116**, 45–64.

Dai M.-H. and Martin J. M. (1995) First data on trace metal level and behaviour in two major Artic river-estuarine systems (Ob and Yeanisey) and in the adjacent Kara Sea, Russia. *Earth Planet. Sci. Lett.* **131**, 127–141.

de Baar H. J. W., de Jong J. T. M., Bakker D. C. E., Löscher B. M., Cornelis V., Bathmann U., and Smetacek V. (1995) Importance of iron for plankton blooms and carbon dioxide drawdown in the Southern Ocean. *Nature* **373**, 412–415.

Déruelle B. and Bourgois J. (1993) Sur la dernière eruption du volcan Hudson (sud Chili, août 1991). *C. R. Acad. Sci. Paris* **316, 2,** 1399–1405.

Diekmann B., Kuhn G., Rachold V., Abelmann A., Brathauer U., Fütterer D. K., Gersonde R., and Grobe H. (2000) Terrigenous sediment supply in the Scotia Sea (Southern Ocean): Response to Late Quaternary ice dynamics in Patagonia and the Antarctic Peninsula. *Palaeogeogr. Palaeoclimatol. Palaeoeocol.* **162**, 357–387.

Dong D., Nelson Y. M., Lion L. W., Shuler M. L., and Ghiorse W. C. (2000) Adsorption of Pb and Cd onto metal oxides and organic material in natural surface coatings as determined by selective extractions: New evidence for the importance of Mn and Fe oxides. *Water Res.* **34**, 427–436.

Duce R. A. (1986) The impact of atmospheric nitrogen, phosphorous, and iron species on marine biological productivity. In *The Role of Air-Exchange in Geochemical Cycling* (ed. P. Buat-Ménard), pp. 497–529. D. Reidel, Norwell, MA.

Duce R. A. and Tindale N. W. (1991) Atmospheric transport of iron and its deposition in the ocean. *Limnol. Oceanogr.* **36, 8,** 1715–1726.

Duce R. A., Liss P. S., Merrill J. T., Atlas E. L., Buat-Ménard P., Hinks B. B., Miller J. M., Prospero J. M., Arimoto R., Church T. M., Ellis W., Galloway J. N., Hansen L., Jickells T. D., Knap A. H., Reinhardt K. H., Schneider B., Soudine A., Tokos J. J., Tsunogai S., Wollast R., and Zhou M. (1991) The atmospheric input of trace species to the world ocean. *Global Biochem. Cycles* **5, 3,** 193–259.

Dupré B., Gaillardet J., Rousseau D., and Allègre C. J. (1996) Major and trace elements of river-borne material: The Congo Basin. *Geochim. Cosmochim. Acta* **60**, 1301–1321.

Ewing M., Eittreim S. L., Ewing J. I., and Le Pichon W. (1971) Sediment transport and distribution in the Argentine Basin, 3. Nepheloid layer and processes of sedimentation. *Phys. Chem. Earth* **8**, 40–77.

Falkowski P. G., Barber R. T., and Smetacek V. (1998) Biogeochemical controls and feedbacks on ocean primary production. *Nature* **281**, 200–206.

Förstner U. and Wittman G. T. W. (1981) *Metal Pollution in Aquatic Environment.* Spring-Verlag, Berlin, Germany.

Fung I. Y., Meyn S. K., Tegen I., Doney S. C., John J. G., and Bishop J. K. B. (2000) Iron supply and demand in the upper ocean. *Global Biogeochem. Cycles* **14, 1,** 281–295.

Gaiero D. M., Probst J. L., Depetris P. J. Leleyter L., and Kempe S. (2002) Riverine transfer of heavy metals from Patagonia to the Southwesten Atlantic Ocean. *Reg. Environ. Change.* **3**, 51–64.

Gibbs R. J. (1977) Transport phases of transition metals in the Amazon and Yukon Rivers. *Geol. Soc. Am. Bull.* **88**, 829–843.

Ginoux P., Chin M., Tegen I., Prospero J. M., Holben B., Dubovik O., and Lin S.-J. (2001) Source and distribution of dust aerosols simulated with the GOCART model (2001). *J. Geophys. Res.* **106**, 20255–20273.

Global Volcanism Network Bulletin (1991) Smithsonian Institution, Washington D.C. **16, 7,** 2–4.

Goldschmidt V. M. (1933) Grundlagen der quantitativen Geochemie. *Fortschr. Minerl. Krist. Petrol.* **17**, 112.

Guerzoni S., Chester R., Dulac F., Herut B., Lo'ffe-Pilot M.-D., Measures C., Migon C., Molinaroli E., Moulin C., Rossini P., Saydam C., Soudine A., and Ziveri P. (2001) The role of atmospheric deposition in the biogeochemistry of the Mediterranean Sea. *Prog. Oceanogr.* **44**, 147–190.

Hoffmann A. (1999) Kurtfristige Klimaschwankugen im Scotiameer und Ergebnisse zur Kalbungsgeschichte der Antarktis während der letzten 200.000 Jahre. *Ber. Polarforsch.* 345 Bremerhaven.

Horowitz A. J. (1991) *A Primer on Sediment-Trace Element Chemistry.* Lewis Publishers. QE516. T85 H67.

Huang W. W., Zhang J., and Zhou Z. H. (1992) Particulate element inventory of the Huanghe (Yellow River): A large, high turbidity river. *Geochim. Cosmochim. Acta* **56**, 3669–3680.

Iriondo M. (2000) Patagonian dust in Antarctica. *Quat. Int.* **68–71**, 83–86.

Jenne E. A. (1968) Control on Mn, Fe, Co, Ni, Cu and Zn concentrations in soils and water. The significant role of Mn- and Fe-oxides. *Am. Chem. Soc. Adv. Chem. Serv.* **73**, 337–387.

Jenne E. A. (1976) Trace elements sorption by sediments and soils-sites and processes. In *Symposium on Molybdenum, Vol. 2* (eds. W. Chappell and K. Petersen), pp. 425–553. Marcel Dekker, New York.

Klaus A. and Ledbetter M. T. (1988) Deep-sea sedimentary processes in the Argentine Basin revealed by high-resolution seismic records (3.5 kHz echograms). *Deep-Sea Res.* **35, 6,** 899–917.

Kumar N., Anderson R. F., Mortlock R. A., Froelich P. N., Kubik P., Dittrich-Hannen B., and Suter M. (1995) Increased biological productivity and export production in the Glacial Southern Ocean. *Nature* **378**, 675–680.

Lantzy R. J. and Mackenzie F. T. (1979) Atmospheric trace metals: Global cycles and assessment of man's impact. *Geochim. Cosmochim. Acta* **43**, 511–525.

Leleyter L. and Probst J.-L. (1999) A new sequential extraction procedure for the speciation of particulate trace elements in river sediments. *Int. J. Environ. Anal. Chem.* **73, 2,** 109–128.

Lienemann C.-P., Taillefert M., Perret D., and Gaillard J.-F. (1997) Association of cobalt and manganese in aquatic systems: Chemical and microscopic evidence. *Geochim. Cosmochim. Acta* **61**, 1437–1997.

Ludwig W. and Probst J.-L. (1998) River sediment discharge to the oceans: Present-day controls and global budgets. *Am. J. Sci.* **298**, 265–295.

Martin J. H., Gordon R. M., and Fitzwater S. E. (1991) The case for iron. What controls phytoplankton production in nutrient rich areas of open sea? *Limnol. Oceanogr.* **36**, 1793–1802.

McLennan S. (1995) Sediments and soils: Chemistry and abundances. In *Rock Physics and Phase Relations. A Handbook of Physical Constants*, pp. 8–20. AGU Reference Shelf 3.

Migon C., Journel B., and Nicolas E. (1997) Measurement of trace metal wet, dry and total atmospheric fluxes over the Ligurian Sea. *Atmos. Environ.* **31**, 889–896.

Milliman J. D. and Meade R. H. (1983) World-wide delivery of river sediments to the ocean. *J. Geol.* **1**, 1–21.

Naranjo J. A. and Stern C. R. (1998) Holocene explosive activity of Hudson volcano, southern Andes. *Bull. Volcanol.* **59**, 291–306.

Neftel A., Oeschger A. H., Staffelabch Y., and Stauffer B. (1988) CO_2 record in the Byrd ice core 50,000-5,000 years BP. *Nature* **331**, 609–611.

Orange D., Gac J. Y., Probst J.-L., and Tanre D. (1990) Mesure du dépôt au sol des aérosol désertiques. Une methode simple de prélèvement: Le capteur pyramidal. *C. R. Acad. Sci. Paris* **311**, 2, 167–172.

Piccolo M. C. and Perillo G. M. E. (1999) Estuaries of Argentina: A review. In *Estuaries of South America: Their Geomorphology and Dynamics* (eds. G. M. E. Perillo, M. C. Piccolo, and M. Pino Quivira), pp. 101–132. Springer-Verlag, Berlin, Germany.

Pierce J. W. and Siegel F. R. (1979) Suspended particulate matter on the southern Argentine shelf. *Mar. Geol.* **29**, 73–91.

Pinet P. and Souriau M. (1988) Continental erosion and large scale relief. *Tectonics* **7**, 563–582.

Prospero J. M., Ginoux P., Torres O., Nicholson S. E., and Gill T. (2002) Environmental characterization of global sources of atmospheric soil dust identified with NIMBUS-7 TOMS absorbing aerosol products. *Rev. Geophys.* **40**, 1, 1002.

Pye K. (1989) *Eolian Dust and Dust Deposits*. Academic/Harcourt, New York.

Ramsperger B., Peinemann N., and Stahr K. (1998) Deposition rates and characteristics of aeolian dust in the semi-arid and sub-humid regions of the Argentinian Pampa. *J. Arid Environ.* **39**, 467–476.

Romo-Kröger C. M., Morales J. R., Dinator M. I., and Llona F. (1994) Heavy metals in the atmosphere coming from a copper smelter in Chile. *Atmos. Environ.* **28**, 4, 705–711.

Rostagno C. and Del Valle H. (1988) Mounds associated with shrubs in aridic soils of north-eastern Patagonia: Characteristics and probable genesis. *Catena* **15**, 347–385.

Salomons W. and Förstner U. (1984) *Metals in the Hydrocycle*. Springer-Verlag, New York.

Scasso R., Corbella H., and Tiberi P. (1994) Sedimentological analysis of the tephra from the 12-15 August 1991 eruption of Hudson volcano. *Bull. Volcanol.* **56**, 121–132.

Schnack E. J. (1985) Argentina. In *The World's Coastline* (eds. E. Bird and M. Schwartz), pp. 69–78. Van Nostrand Reinhold Co, New York.

Sholkovitz E. E. and Copland D. (1981) The coagulation, solubility and adsorption properties of Fe, Mn, Cu, Ni, Cd, Co and humic acids in river water. *Geochim. Cosmochim. Acta* **45**, 181–189.

Sholkovitz E. R., Boyle E. R., and Price N. B. (1978) Removal of dissolved humic acid and iron during estuarine mixing. *Earth Planet. Sci. Lett.* **40**, 130–136.

Smellie J. L. (1999) The upper Cenozoic tephra record in the south polar region: A review. *Global Planet. Change* **21**, 51–70.

Stumm W. and Morgan J. J. (1996) *Aquatic Chemistry: Chemical Equilibria and Rates in Natural Waters*. 3rd ed. Wiley Interscience, New York.

Taylor S. R. and McLennan S. M. (1985) *The Continental Crust: Its Composition and Evolution*. Blackwell, Oxford, UK.

Taylor S. R., McLennan S. M., and McCulloch M. T. (1983) Geochemistry of loess, continental crustal composition and crustal model ages. *Geochim. Cosmochim. Acta* **47**, 1897–1905.

Tegen I. and Fung I. (1994) Modeling of mineral dust in the atmosphere: Sources, transport, and optical thickness. *J. Geophys. Res.* **99**, 22897–22914.

Tessier A. and Campbell P. G. C. (1987) Partitioning of trace metals in sediments: Relationship with bioavailability. *Hydrobiologia* **149**, 43–52.

Tessier A., Fortin D., Belzile N., DeVitre R. R., and Leppard G. G. (1996) Metal sorption to diagenetic iron and manganese oxhydroxides and associated organic matter: Narrowing the gap between field and laboratory measurements. *Geochim. Cosmochim. Acta* **60**, 387–404.

Trefry J. H. and Presley B. J. (1976) Heavy metal transport from the Mississippi River to the Gulf of Mexico. In *Marine Pollution Transfer* (eds. H. L. Windom and R. A. Duce), pp. 39–76. Health and Co, Lexington.

Ure A. M. and Berrow M. L. (1982) The chemical constituents of soils. In *Environmental Chemistry* (ed. H. J. M. Bowen), pp. 94–202. R. Soc. Chem, Burlington House, London.

Urien C. M. and Ewing M. (1974) Recent sediments and environment of southern Brazil, Uruguay, Buenos Aires, and Rio Negro Continental shelf. In *The Geology of Continental Margins* (eds. Burks and Drake), pp. 157–177. Springer, New York.

Viers J., Duprè B., Braun J.-J., Deberdt S., Angeletti B., Ngoupayou J. N., and Michard A. (2000) Major and trace element abundances, and strontium isotopes in the Nyong basin rivers (Cameroon): Constrains on chemical weathering processes and elements transport mechanisms in humid tropical environments. *Chem. Geol.* **169**, 211–241.

Walter H. J., Hegner E., Diekmann B., Kuhn G., and Rugters van der Loeff M. M.. (2000) Provenance and transport of terrigenous sediment in the South Atlantic Ocean and their relations to glacial and interglacial cycles: Nd and Sr isotopic evidence. *Geochim. Cosmochim. Acta* **64**, 3813–3827.

Wilson H. D. B. and Laznicka B. (1972) Copper belts, lead belts and copper-lead lines of the world. *Int. Geol. Cong. 24th*, Section 4, pp. 37–59, Montreal.

Winslow M. A. (1982) The structural evolution of the Magallanes Basin and neotectonics in the southernmost Andes (ed. C. Craddock). Antarctic Geoscience International Union of Geological Sciences Series B N° 4, pp. 143–154. University of Wisconsin Press, Madison.

Wolff E. W., Suttie E. D., and Peel D. A. (1999) Antarctic snow record of cadmium, copper, and zinc content during the twentieth century. *Atmos. Environ.* **33**, 1535–1541.

Yeats P. A. and Bewers J. M. (1982) Discharge of metals from St. Lawrence River. *Can. J. Earth Sci.* **19**, 982–992.